Thesis for the Degree of Master of Engineering

High Throughput Multi-User Visible Light Communication with LEDs for High-speed Wireless Data Networks

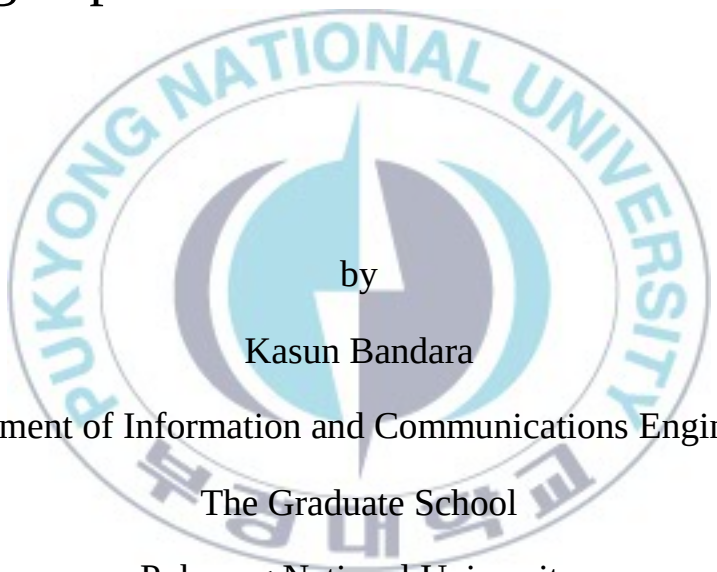

by

Kasun Bandara

Department of Information and Communications Engineering

The Graduate School

Pukyong National University

February 2014

High Throughput Multi-User Visible Light Communication with LEDs for High-speed Wireless Data Networks

고속 무선 데이터 네트워크를 위한 LED기반의 고수율 다중사용자 가시광통신

Advisor: Prof. Yeon-Ho Chung

by

Kasun Bandara

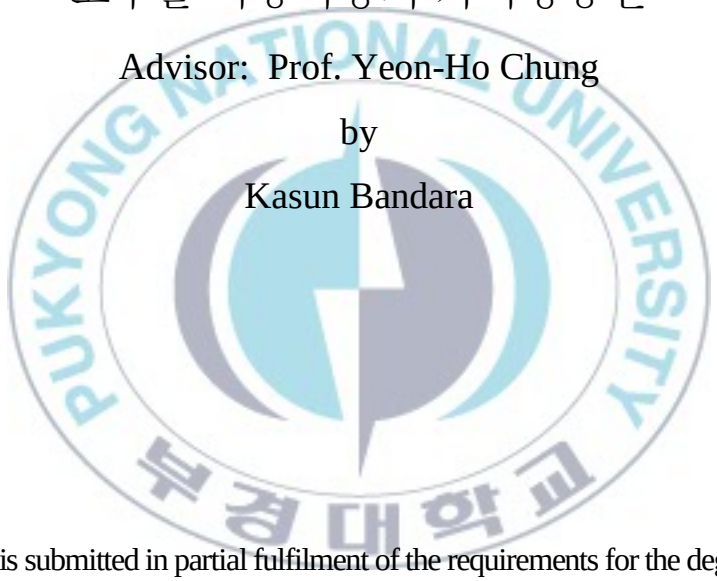

A thesis submitted in partial fulfilment of the requirements for the degree of

Master of Engineering

in Department of Information and Communications Engineering,

The Graduate School,

Pukyong National University

February, 2014

High Throughput Multi-User Visible Light Communication with LEDs for High-speed Wireless Data Networks

A dissertation

by

Kasun Bandara

Approved by:

_____

Professor Deock-Ho Ha,
(Chairman)

_____

Professor Kyu-Chil Park,
(Member)

_____

Professor Yeon-Ho Chung,
(Member)

February, 2014

Table of Contents

List of Figures

List of Tables

List of Abbreviations

AWGN ····· Additive White Gaussian Noise
BER ····· Bit Error Rate
CCDF ····· Complementary Cumulative Distribution Function
CDF ····· Cumulative Distribution Function
CIE ····· International Commission on Illumination
CSK ····· Color Shift Keying
CT ····· Companding Transform
DAPPM ····· Differential Amplitude Pulse Position Modulation
DD ····· Direct Detection
DFE ····· Decision Feedback Equalizer
DFTS ····· Discrete Fourier Transform-Spread
FBF ····· Feed Back Filter
FFF ····· Feed Forward Filter
FOV ····· Field Of View
I.I.D ····· Independent and Identically Distributed
ID ····· Identification
IM ····· Intensity Modulation
ISO ····· International Organization for Standardization
LED ····· Light Emitting Diode
LMS ····· Least Mean Square
LOS ····· Line-Of-Sight
M-PAM ····· Multi-Level Pulse Amplitude Modulation
MU ····· Multi-User
OAP ····· Outage Area Probability
OCDMA ····· Optical Code Division Multiple Access

OFDM····· Orthogonal Frequency Division Multiplexing
OOK·····On-Off-Keying
PAM····· Pulse Amplitude Modulation
PAPR····· Peak-To-Average Power Ratio
PD ····· Photo Detector
PPM ····· Pulse Position Modulation
PSD····· Power Spectrum Density
RCLED ·····Resonant Cavity LED
RF·····Radio Frequency
RGB ····· Red-Green-Blue
RLL·····Run Length Limited
RLS·····Recursive Least Square
rms·····Root Mean Square
ROC ····· Random Optical Codes
RSI····· Received Signal Intensity
TS·····Training Sequence
V-I ·····Voltage-Current
VLC ····· Visible Light Communication
ZF·····zero forcing

Acknowledgement

First and foremost, I would like to present my utmost gratitude to my supervisor, Professor, Yeon-Ho Chung for providing me with the opportunity to pursue the Master's degree in Mobile Transmission Systems (MTS) Laboratory, Pukyong National University, Busan, South Korea. His thorough supervision and appreciable support have enabled me to materialize my objective of successful completion of Master's degree in Korea.

I would like to thank the members in the Office of International Relations and other department offices in Pukyong National University for the facilities and supports given me for the stay in Korea.

I would like to thank and appreciate my colleagues in the MTS laboratory and the other friends I met in Korea for their support given me in one way or another throughout my precious life in Korea.

Last but not least, my sincere love and thanks to my mother and father for their words of encouragement and love which brought me faith and happy life while staying away from home.

Kasun Bandara

Department of Information & Communications Engineering

Pukyong National University, Busan, South Korea

High Throughput Multi-User Visible Light Communication with LEDs for High-speed Wireless Data Networks

Kasun Bandara

Department of Information and Communications Engineering, The Graduate School, Pukyong National University

Abstract

With the advancement of light emitting diode (LED) technology, visible light communication (VLC) emerged as a novel way of providing data communication. Using visible light as the communication medium, VLC possesses many advantages over conventional RF communications, such as large unlicensed spectral bandwidth, usability at RF-prohibited areas. Since data transmission is done via LEDs using intensity modulation techniques, VLC is able to provide data rates faster than the LED switching rate, which is a several hundred of Megahertz. This thesis provides a design of an indoor multi-user (MU) VLC system and it analyses the system addressing some of the important issues in indoor VLC. Moreover, the thesis provides a fundamental analysis of the VLC system in the aspects of indoor illumination, power reception and channel dispersion in the indoor environment. The ultimate target of designing the indoor MU-VLC system is achieved by conducting the study in four sections.

In the first study, a decision feedback equalizer (DFE) with adaptive recursive least square (RLS) algorithm is analyzed for the reduction in the length of the training sequence (TS) used in the DFE. The reduced TS length allows more data bits to be transmitted, and hence facilitates higher bit rate. The use of RLS-DFE also enables the VLC system to reduce the multipath induced inter-symbol interference (ISI) that helps to increase data rate with improved bit error rate performance (BER).

Secondly, the thesis presents the studies on multilevel pulse amplitude modulation (PAM) with RLS-DFE for VLC systems. The PAM scheme supports higher throughput and

the RLS-DFE facilitates to use fewer bits for the TS, so that the data rate can be increased over the limitation of LED modulation speed. The simulation results of the outage area probability show that the VLC system supports high data rate transmission at nearly error-free rates for most areas in indoor environments.

As a promising way of reducing the multipath effects, the third study employs orthogonal frequency division multiplexing (OFDM) in the indoor VLC system. The original OFDM signal inherently composed with signal peaks with high power, causing high peak-to-average power ratio (PAPR). At the transmission of this high PAPR signal, the LEDs are overheated due to the limited output power and the transmitted signal is also distorted due to the nonlinear characteristics of the LEDs. Therefore, it is crucial to reduce the PAPR of the OFDM signal before it is fed into the LEDs. The third study of the thesis presents the analysis of μ-law CT and exponential CT schemes in terms of PAPR reduction and it also proposes a novel CT scheme that can be efficiently used for the reduction of PAPR in VLC-OFDM. The simulations comparatively analyze the performances of each CT scheme with other CT schemes. It shows from the results that the CT schemes perform with significant PAPR reduction in VLC-OFDM signal providing excellent BER performances.

The MU-VLC system is designed in the last study, proposing a novel MU-VLC system exploiting the visible light spectrum. The proposed scheme is defined as color-clustered multiuser VLC and the study makes sure that the MU-VLC system is complete in that it encompasses transmission and detection methods for multiple user access, while ensuring a color-controlled flicker free illumination. The simulations demonstrate that the proposed MU-VLC system provides an efficient multiuser VLC platform with significant performances over various transmission scenarios.

1. Introduction

1.1. Visible Light Communication

Visible light is identified as a better candidate for wireless communications as it has several advantages over other electromagnetic media. Among these, no interference with other electromagnetic spectra, the least harm to human health, usability in electromagnetic prohibited areas such as airplane cabins and hospitals, isolated transmission and the large unregulated spectral range are noteworthy, compared with radio waves. Not surprisingly, with these inherent advantages, visible light is regarded as a next generation wireless communication medium [1], and many researchers and the commercial electronic industry are much attracted to visible light communication (VLC). With extensive researches and developments conducted over a decade, VLC systems have largely been focused on providing point-to-point communication links with substantial performances [1-4].

A VLC system transmits data utilizing an intensity modulation (IM) technique that changes light intensity according to the transmitted signal. Preliminarily, VLC utilizes three IM schemes; on-off-keying (OOK), pulse position modulation (PPM) and color-shift keying (CSK) [5]. Moreover, modified schemes of these primary schemes, such as differential amplitude PPM (DAPPM) [6], differential PPM [7] are also applicable for VLC. For the performance improvement over dispersive channels, higher complex modulation schemes such as orthogonal frequency division multiplexing (OFDM) are also used [3]. At the receiver, the light intensity is converted into an electrical signal using a photo detector (PD), i.e. direct detection (DD). In the VLC systems, light emitting diodes (LEDs) are the most widely used device to transmit the IM signal, after Y. Tanaka *et al.* proposed an

indoor VLC system that utilizes white LEDs [1]. With the rapid development of technology, LEDs achieved an enormously fast switching speed that can be advantageously used in VLC systems to modulate high-speed data. Moreover, LEDs were found to be significantly efficient and environmentally friendly over incandescent bulbs which have a wide infrared emission, and fluorescent lamps that contain poisonous mercury layer. These advantages let LEDs to be the next generation general source of illumination [8] and to be used as a data communication device simultaneously.

1.2. Motivations and Research Objectives

In the study of this research, following aspects are considered for the improvement of indoor VLC systems.

- Although there are a number of researches and developments in point-to-point VLC links, the requirement for an efficient point-to-multipoint or multi-user (MU) VLC system has not been addressed well in the literature yet. As a fast and efficient communication scheme, VLC should be able to facilitate high-speed MU links as well.
- Visible light, as well as the other electromagnetic radiation, travels in straight paths in free space. This causes VLC systems to have line-of-sight (LOS) communication preferable in most of the time. However, in indoor environments, reflection paths also contribute to the received signal strength. As a result of the multipath propagation from reflection paths and LOS paths from multiple transmitters, indoor VLC suffers from inter-symbol-interference at high-speed data transmission. Therefore, it is crucial in indoor VLC to study the methods to reduce multipath effects in order for higher transmission rates.

- Regarding the wireless network usage among the users, there is an increasing demand for high-speed data transmission. Although LEDs have a fast switching capability for IM of data, the modulation rate should not be limited by the LED switching speed. This leads to explore new methods to improve throughput under the LED switching speed limitations.
- As a promising technique to combat with multipath effects, OFDM can be used in indoor VLC systems as well. However, the inherent high peak-to-average power ratio (PAPR) of OFDM signal adversely affects the LEDs due to the nonlinear characteristics and limited output power of the LEDs. Therefore the PAPR should be reduced before the OFDM signal is fed into LEDs. Although there are many techniques proposed for PAPR reduction, the PAPR reduction in VLC-OFDM should be comprehensively analyzed since the VLC-OFDM signal is a real-valued unipolar signal. Moreover, the power requirements in the LEDs should also be considered when proposing new criteria for PAPR reduction in VLC-OFDM.

With these motivations, the study in this thesis considers the following objectives.

i. To mitigate the multipath induced ISI in indoor VLC.
ii. To improve throughput of VLC systems for high-speed transmission.
iii. To reduce the adverse effects of high PAPR on the VLC-OFDM signal caused by LED characteristics.
iv. To design an efficient and complete MU access scheme for indoor VLC.

1.3. Chapter Organization

The remaining chapters in this thesis are outlined as follows. Chapter 2 describes the VLC system designed for indoor environments. The indoor VLC system is analyzed for fundamental performances such as lighting and illumination, power reception and channel dispersion. The experimental studies are presented in Chapter 3. In the subsections that describe each experiment, the theoretical background of the research is first presented and the simulation results are then discussed. Chapter 4 draws conclusions based on the studies considering all the experimental analyses.

2. Indoor VLC System Design

The study is based on an indoor VLC system that simultaneously provides illumination and data communication. Generally, an indoor VLC system uses multiple LED lighting sources for the provision of sufficient illumination, which is one of the basic requirements of indoor VLC systems. Inside a typical office room, these light sources are installed on the ceiling apart from each. Moreover, a general lighting system should provide illumination without flickering that would be harmful for human eyes. The study considers techniques that mitigate illumination flickering for a safe lighting system.

2.1. VLC Channel Model

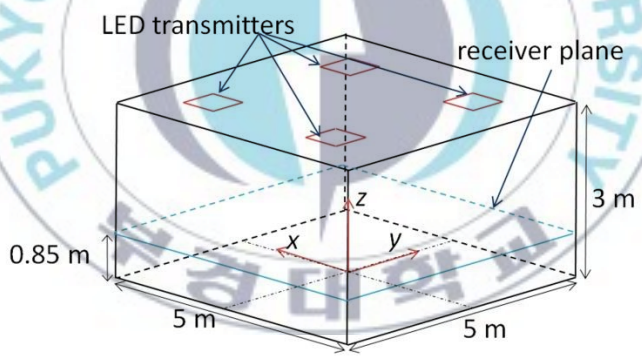

Figure 2.1. Indoor VLC environment considered.

The study considered an indoor channel model. As shown in Figure 2.1, the indoor environment considered in the investigation is an empty room with dimensions 5 × 5 × 3 m^3. A *xyz* coordinate system is defined on the floor such that the origin is at the center of the floor. There are four LED

transmitters placed on the ceiling of the room at the positions given in Figure 2.2. The centers of the transmitters are (1.25,1.25,3), (-1.25,1.25,3), (1.25,-1.25,3), (-1.25,-1.25,3) and the receiver is considered to be on the receiver plane 0.85m above the floor. The walls of the room are considered to be reflective surfaces with 0.8 reflection coefficient.

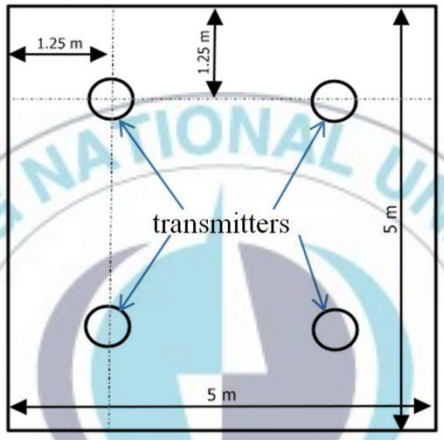

Figure 2.2. Positions of the transmitters.

2.2. Indoor Illumination Analysis

The illumination expresses the brightness of an illuminated surface [9]. It is assumed that all the LEDs and reflection points on the walls are Lambertian, That is, the luminous intensity at an irradiance angle θ has a cosine variation [1]. The luminous intensity at an angle θ is given by

$$I(\theta) = I\cos^{m}(\theta) \tag{2.1}$$

Here, I is the center luminous intensity of an LED, and m is the order of Lambertian emission and is given by the following function of an LED's semi-angle at half power θ_{hp}.

$$m = -ln(2)/ln(cos\ \theta_{hp}) \tag{2.2}$$

When the incident angle on the receiver is φ, the illumination, E, at a receiver position in D distance from the source is given by

$$E = I\ cos^m(\theta)/D^2 cos(\varphi) \tag{2.3}$$

Table 2.1. Simulation parameters of the VLC system.

	Parameter	Value
Room	Size	$5 \times 5 \times 3$ m^3
	Reflection coefficient of walls	0.8
Source	Location of LEDs	(1.25,1.25,3), (-1.25,1.25,3), (1.25,-1.25,3), (-1.25,-1.25,3)
	θ_{hp}	70°
	Output power of an LED	20 mW
	Number of LEDs per Transmitter	27
	Center luminance intensity of LED	150 lx
Receiver	Receiver plane above the floor	0.85 m
	Effective are (A)	1 cm^3
	Ψ_{FOV}	60°
	Elevation	90°

The illumination on the receiver plane is simulated according to the system parameters shown in Table 2.1. The illumination distribution is shown in Figure 2.3. It can be seen in Figure 2.3 that the illuminance varies from about 400 lx to 1400 lx. The International Organization for Standardization (ISO) standardizes the illumination required for general

lighting. According to these standards, an illuminance of 300 to 1500lx is required for office work. Therefore, the considered LED transmitter arrangement in this study is able to provide sufficient illumination for the indoor environment.

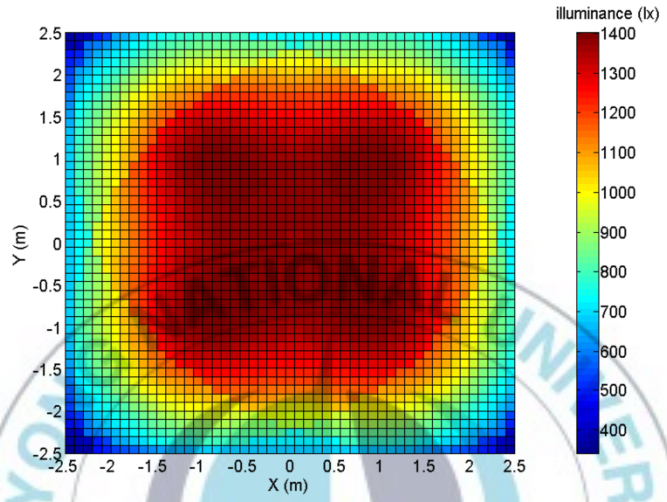

Figure 2.3. Illumination distribution on the receiver plane.

2.3. Received Power Analysis

The receiver receives the IM signals from LOS paths and reflections from the walls. If the channel DC gains on LOS paths and reflected paths are H_{LOS} and H_r, respectively, the received optical power, P_r, is calculated as the product of DC gains and the transmitted power , P_t,. The received power from S LEDs and R reflection points is calculated as [1].

$$P_r = \sum^{S} \left\{ P_t H_{LOS} + \sum_{r=1}^{R} P_t H_r \right\} \tag{2.4}$$

Since the power received from the incidence angles less than the field of view (FOV), Ψ_{FOV}, of the PD, H_{LOS} and H_r are calculated for $0<\varphi<\Psi_{FOV}$ by

the following standard equations using the propagation model shown in Figure 2.4.

$$H_{LOS} = \frac{(m+1)A}{2\pi D_d^2} cos^m(\theta)\, cos(\varphi)\, T_s(\varphi) g(\varphi) \tag{2.5}$$

$$H_r = \frac{(m+1)dA_r}{2\pi^2 D_1^2 D_2^2} \rho cos^m(\theta)\, cos(\alpha)\, cos(\beta)\, cos(\varphi)\, T_s(\varphi) g(\varphi) \tag{2.6}$$

Here $T_s(\varphi)$ is the optical filter gain and $g(\varphi)$ is the gain of the optical/electrical converter and for $0<\varphi<\Psi_{FOV}$, $g(\varphi)$ is given by

$$g(\varphi) = \frac{n^2}{sin^2(\Psi_{FOV})} \tag{2.7}$$

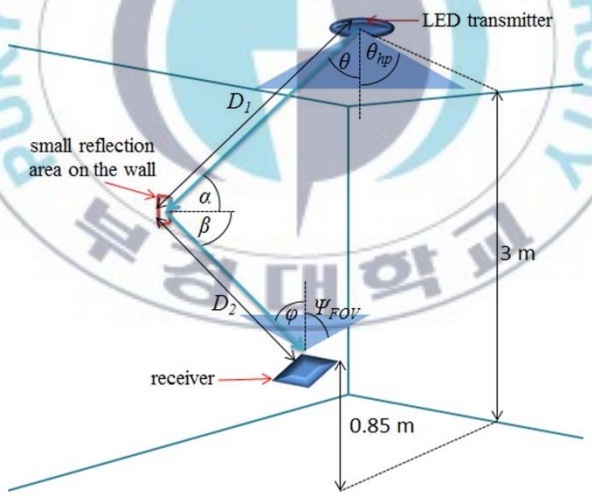

Figure 2.4. VLC propagation model.

Moreover, A is the effective area of the optical detector, dA_r is the small reflective area on the wall and ρ is the reflectivity at the wall. As shown in Figure 2.4, D_1 and D_2 are the distance between the transmitter and the

reflection point, and between the reflection point and the receiver respectively. α is the angle of incidence on the reflective point, β is the angle of irradiance to the receiver, θ is the angle of irradiance to the reflective point.

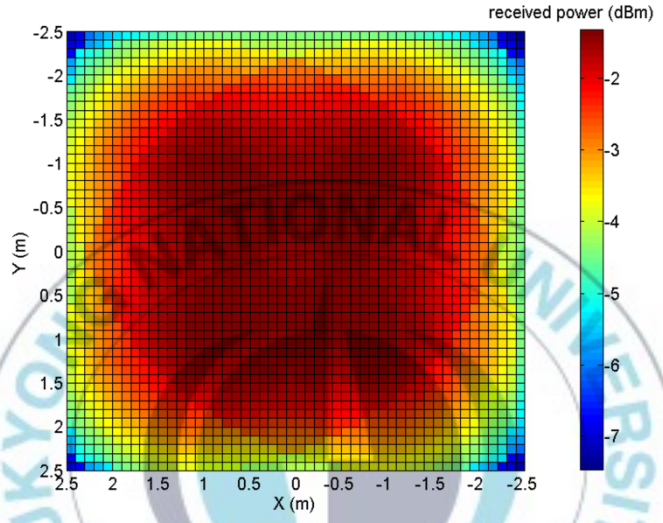

Figure 2.5. Total received power distribution.

Figure 2.5 shows the total received power distribution on the receiver plane. Since the optical power is proportional to the light intensity, the received power distribution has a similar pattern with the illumination distribution on the receiver plane. Based on the illumination and power provided by the LEDs, the designed transmitter arrangement can be confirmed to be sufficient for the indoor VLC system.

2.4. Impulse Response and Delay Spread

The optical wireless channel is represented as:

$$y(t) = R\,x(t) \otimes h(t) + n(t) \tag{2.8}$$

where $y(t)$ represents the received signal, $x(t)$ is the transmitted signal, $h(t)$ is the channel impulse response, $n(t)$ is additive white Gaussian noise (AWGN) and the symbol $\otimes$ represents convolution. R is the optical/electrical convergence efficiency at the PD.

The VLC channel can be described by its frequency response $H(f)$, which is the Fourier transform of the impulse response of the channel $h(t)$. That is

$$H(f) = \int_{-\infty}^{\infty} h(t) e^{-j2\pi f t} dt \tag{2.9}$$

To simulate the channel impulse response, we used the recursive method [10]. The obtained impulse response at the receiver point (0.1,2.1,0.0) is shown in Figure 2.6. We selected the bin width as 0.2 ns. The peaks of the impulse response are generated according to the travel distance of light rays.

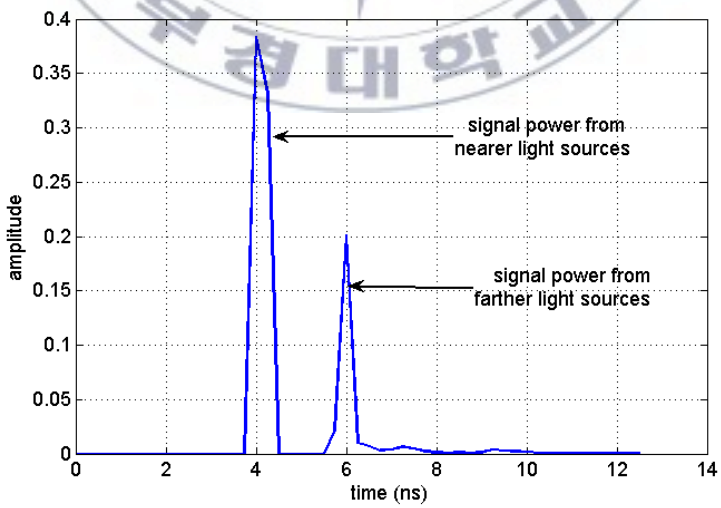

Figure 2.6. Impulse response of the channel at (0.1, 2.0, 0.0).

Another important parameter characterizing a wireless multipath channel is the root mean square (rms) delay spread. Since there are visible light propagation paths arriving from the reflections on walls as well as from the multiple LEDs, VLC systems usually suffer from channel dispersion caused by the delay spread. Therefore, the channel impulse response depends on the location of the receiver under fixed transmitters as shown in (2.5) and (2.6). The VLC channels are considered as quasi-static channel and hence the rms delay spread also depends on the location of the receiver [11]. If the discrete quantities are considered, the relation of the channel DC gain, H, and the impulse response, $h(n)$, can be given as

$$H = \sum_{n} h(n) \tag{2.10}$$

The rms delay spread is given by [12]

$$\tau_{RMS} = \sqrt{\frac{\sum_n (n-\tau)^2 h^2(n)}{\sum_n h^2(n)}} \tag{2.11}$$

where τ is the mean delay given by

$$\tau = \frac{\sum_n n h^2(n)}{\sum_n h^2(n)} \tag{2.12}$$

In order to analyze the error performance of the VLC system under channel dispersions, the rms delay spread distribution is simulated on the receiver plane. The simulation results are shown in Figure 2.7. It can be observed in Figure 2.7 that the rms delay spread over most of the indoor area is between 1 and 1.2ns.

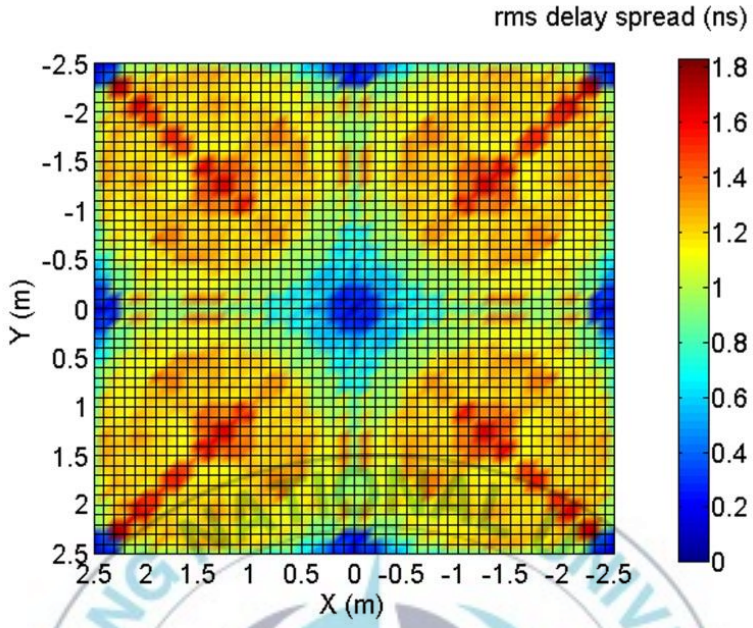

Figure 2.7. rms delay spread distribution on the receiver plane.

3. Performance Analysis of the Indoor VLC System

As described in Chapter 1, the target of this study is to develop a high-speed indoor MU-VLC system with the fulfilled objectives given. In order to materialize the objectives, several experiments were performed on the indoor VLC system described in Chapter 2.

3.1. Indoor VLC with RLS-DFE

As formerly described, the indoor environment uses several LED light sources. When these sources simultaneously transmit signals, it results in multipath propagation of the signals. Due to the multipath signal propagation, transmitted bits may overlap at the receiver and this overlap leads to ISI. It has been shown that the bit error rate (BER) performance of an indoor wireless optical communication system is significantly degraded by the effects of ISI [13].

Zero forcing decision feedback equalizers (ZF-DFE) have been used with wireless infrared channels to overcome the effect of ISI [14, 15]. In those works, it was assumed that the impulse response is known to the receiver. However, the impulse response of the visible light channels is quasi-static since the receiver is usually mobile [16]. The recursive least square (RLS) adaptive algorithm is a well-known algorithm used in dispersive mobile radio channels. A recent study has shown that the RLS algorithm can be used with an LED based identification (LED-ID) system [17]. It has also shown the BER performances of the LED-ID system with several values of rms delay spreads and sampling rates.

However, the length of the training sequence used in the equalizer is a considerable issue in association with energy efficiency in both the transmitter and the receiver. Recently, a decision feedback equalizer with

least mean square (LMS) algorithm has been proposed for indoor VLC systems to mitigate the ISI problem [16, 18]. In this experiment, it is shown that with the RLS algorithm of the DFE, the length of the training sequence can be reduced much more than that used for the LMS algorithm as suggested in previous works. Moreover, the BER performance can be improved considerably.

3.1.1.Principle of Recursive Least Square Decision Feedback Equalizer

The basic idea behind DFE is that once an information symbol has been detected and decided, the ISI can be estimated and subtracted before the detection of subsequent symbols. The DFE can be realized in either the direct transversal form or as a lattice filter. The direct form is shown in Figure 3.1 [18, 19].

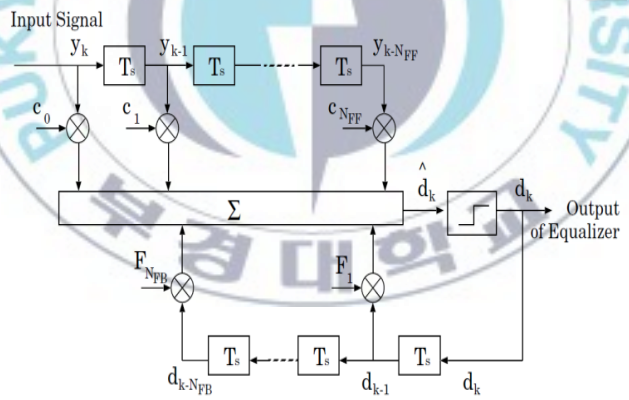

Figure 3.1. Block diagram of a decision feedback equalizer.

It consists of a feed forward filter (FFF) and feedback filter (FBF). The FBF is driven by the decisions on the output of the detector, and its coefficients can be adjusted to cancel the ISI on the current symbol from past

detected symbols. The equalizer has N_{FF}+1 taps in the FFF and N_{FB} taps in the FBF. The output of the filter is given by [18, 19]

$$\hat{d}_k = \sum_{n=0}^{N_{FF}} c_n^* y_{k-n} + \sum_{i=1}^{N_{FB}} F_i^* d_{k-i} \tag{3.1}$$

Here c_n^* and y_n are tap gains and inputs to the FFF and F_i^* are tap gains for the FBF. d_i (i<k) is the previous decision made by the equalizer on the detected signal. That is, $\hat{d}_k$ is obtained using (3.1). d_k along with the previous decisions d_{k-1}, d_{k-2},… are fed back into the equalizer and $\hat{d}_{k+1}$ is obtained [18].

Since the channel is unknown to the receiver, the adaptive algorithm changes the filter weights according to the varying channel. The RLS adaptive algorithm used in this study, recursively finds the filter coefficients that minimize a weighted linear least square cost function related to the input signals. This is entirely different from other algorithms such as LMS that minimizes the mean square error. The advantage of using the RLS algorithm is that it converges more quickly than other methods at the expense of increased complexity with the square of the number of weights. The RLS algorithm can be summarized as follows.

When the variable n denotes the sequence of iterations, weights $w(n)$ are computed as,

$$w(n) = w(n-1) + \alpha(n) g(n) \tag{3.2}$$

$\alpha(n)$ and $g(n)$ are also calculated as follows.

$$\alpha(n) = d(n) - x^T(n) w(n-1) \tag{3.3}$$

$$g(n) = P(n-1) x^*(n) \{\lambda + x^T(n) P(n-1) x^*(n)\}^{-1} \tag{3.4}$$

$\boldsymbol{P}$ is initially defined as $\boldsymbol{P}(0) = \delta^{-1}I$, where δ is the initialization value, I is the identity matrix of rank p+1 where p is the order of the filter, and λ is the 'forgetting factor' which gives exponentially less weight to older error samples. And then,

$$P(n) = \lambda^{-1}P(n-1) - g(n)x^{T}(n)\lambda^{-1}P(n-1) \tag{3.5}$$

Here $x(n) = \{x(n), x(n\text{-}1), x(n\text{-}2),\ldots, x(n\text{-}p)\}^{T}$ is the input the equalizer. $d(n)$ is the desired output of the equalizer. Furthermore, the symbols * and ^{T} denote the complex conjugate and matrix transpose, respectively.

3.1.2.Performance of the Indoor VLC with RLS-DFE

To prove that the RLS algorithm with DFE for VLC channel can be used to minimize the training sequence length of the data frame, we perform several simulations.

We simulate with a different number of taps in FBF and the FFF of the equalizer and found that the optimum number of taps is 4 in FFF and 2 in FBF. We used the forgetting factor of the RLS algorithm as 0.999 and 0.99 for the initialization parameter for the inverse correlation matrix. We calculated the BER for data rates of 100Mbps, 500Mbps, 1Gbps and 5Gbps. The change of BER with the length of the training sequence is shown in Figure 3.2. We also show the BERs for different data rates. Note that we initially calculate the BER at the receiver position (0.1,2.1,0.0). We use a data frame of 15,000 bits.

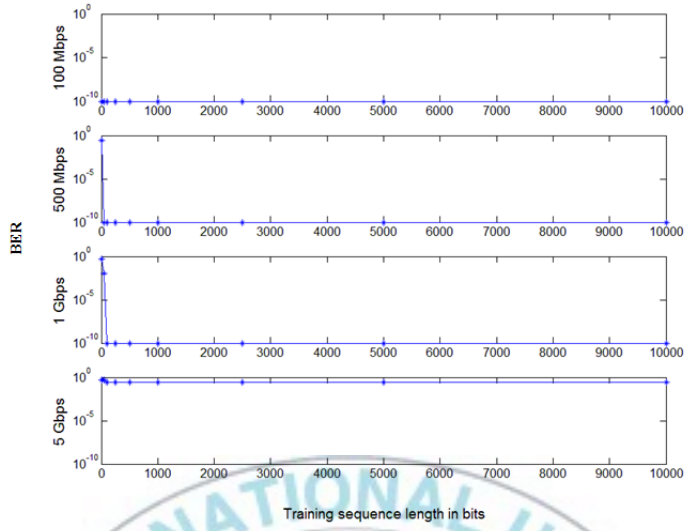

Figure 3.2. BER variations over different data rates according to training sequence length.

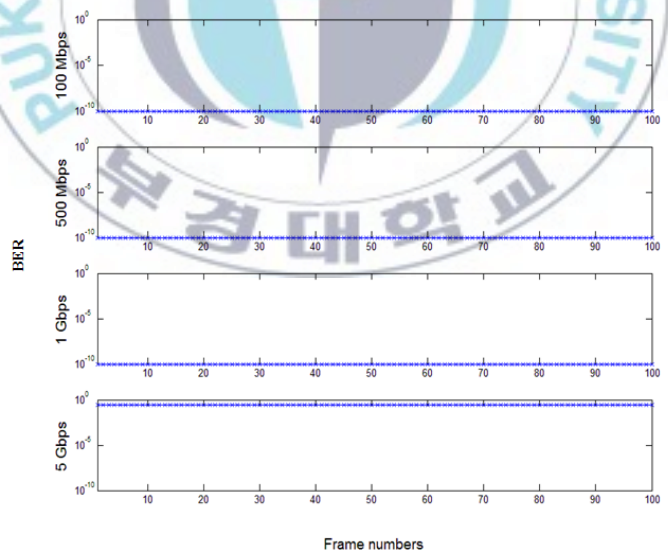

Figure 3.3. BER of the VLC system over different data rates. The training length is 500 bits.

From the results in Figure 3.2, we can see that the BER is stable after 500 bit training sequence. Hence we suggest that the optimum training sequence length is 500 bits. Using the 500 bit training sequence, we calculate BERs for arbitrary data frames of different data rates and showed the results in Figure 3.3. Hence, we can see that the system performance improves greatly with the RLS algorithm of the suggested 500 bit training sequence.

Previous works with the LMS algorithm suggest that the length of the training sequence should be 20,000 bits for 1Gbps [16] or 10,000 bits for 500Mbps [18]. However, with the RLS algorithm, we need only 500 bits up to a data rate of 1Gbps. This is an important advantage in terms of energy efficiency of the transmitter and receiver as well as the whole VLC system.

BER distributions over the working plane with and without the equalizer are shown in Figures 3.4 and 3.5, respectively. For these simulations, we use the suggested training sequence of 500 bits with a data rate of 500Mbps. It can be seen that the BER performance improves significantly.

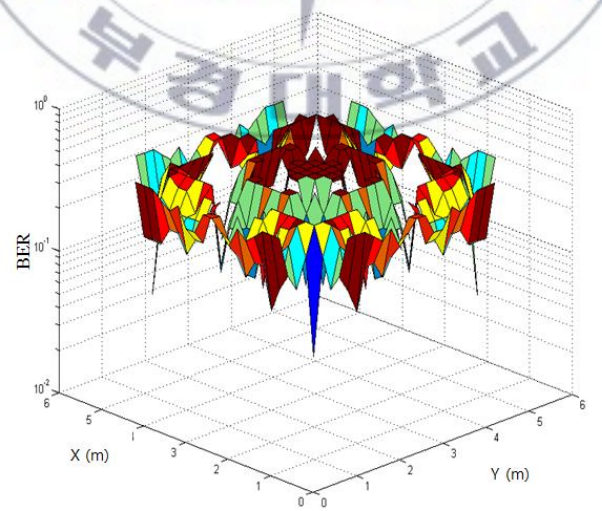

Figure 3.4. BER distribution without the equalizer.

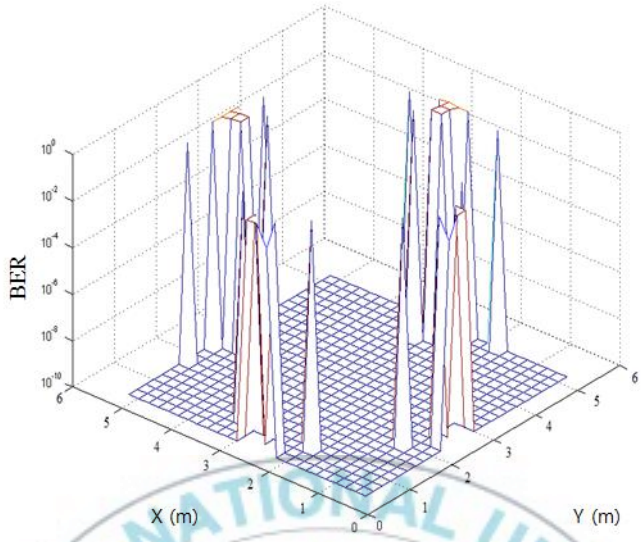

Figure 3.5. BER distribution with the equalizer.

3.2. Multilevel Pulse Amplitude Modulation based VLC

With an increasing demand for very high speed communication systems, VLC suffers from LED switching speed limitations. Typical low cost LEDs can be modulated up to 100Mbps and resonant cavity LEDs (RCLED) can even be modulated up to 500Mbps [20]. On the other hand, the efficient conversion rate of PD is limited to approximately 500MHz. Hence, the PD conversion rate is also a key factor that limits the data rate of a VLC system.

A pulse amplitude modulation (PAM) scheme in VLC has been considered in several works in the past [21]. These works focus on the capacity of the VLC link. However, the LED switching speed limitation which is a practical issue in VLC systems has not been addressed in the literature. And also performance and throughput issues in the PAM-VLC system have yet to be reported.

In this study, we consider an improved VLC system with high data rate and throughput performance, based on the current LED modulation speed

and the PD conversion rate. We employ a multilevel PAM (M-PAM) to increase data rate and attempt to reduce the training sequence (TS) length of an RLS-DFE for throughput improvement. This work assumes that the maximum LED modulation speed and PDs' conversion rate are 500MHz. We develop a 4-PAM VLC system, where we transmit two bits each PAM symbol. Therefore, the system achieves a data rate of 1Gbps.

Using the RLS-DFE receiver in this simulation, we show that system throughput can be increased significantly with the aid of 4-PAM transmission.

3.2.1.Principle of PAM for VLC

Since the maximum modulation speed of the commercially available LEDs (i.e. RCLEDs) is 500Mbps, the maximum data rate will be 500Mbps, if the simple OOK is used.

In M-PAM, M intensity levels are used for IM the data. So that $\log_2 M$ bits are used per M-PAM symbol. In the simulation, 4-PAM is used, that is we transmit data using four intensity levels converting 2 bits (i.e. $\log_2 4$ bits) in one intensity level. Therefore, if the symbol rate is 500Mbps, the actual data rate becomes 1Gbps. We note that the number of intensity levels should be chosen in such a way that it is compatible with the photo detector, because the photo detector should be able to detect and separate the intensity levels accurately.

3.2.2.Performance of 4-PAM and RLS-DFE in indoor VLC

For the present study, we employ a multilevel PAM scheme to increase the data rate in connection with the RLS-DFE receiver.

The block diagram of the simulation is shown in Figure 3.6. We fix the data frame length to 300ms. A data stream of 1Gbps data rate is generated and convolutional coding is performed. After the mapping, the symbols are transmitted through the VLC channel at 500Msymbols/s rate. After the photo detector detects the intensity levels, the symbols are re-generated at the receiver. Then the symbols are equalized and demapped into bits. The numbers of taps used are four taps for FFF and two taps for FBF. The forgetting factor of the RLS algorithm (λ) is set at 0.999 and the initialization parameter of the inverse correlation matrix (δ) is set as 0.99.

The total number of bits in the 4-PAM frame is 30,000 and as suggested in [4], we reserve first 500 bits for the TS. Therefore, we transmit 29,500 data bits (or 14,750 symbols) per data frame, compared with 14,500 transmitted data bits (or 14,500 symbols) in [4].

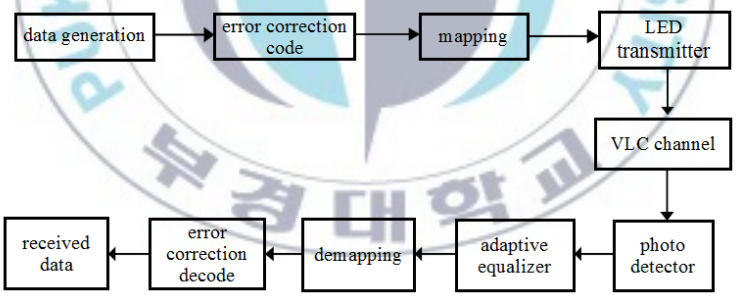

Figure 3.6. Block diagram of the simulation.

First, we calculate the BER with 4-PAM for every receiver position in the room. Figure 3.7(a) shows the results. The maximum BER is found to be 0.5000 and the minimum is 10^{-10}. Average BER over the working plane is 0.0501.

We also obtain the BER distribution for the conventional OOK transmission at the same symbol rate (500 Msymbols/s) with the same 500 bits TS length for the same data frame. Note that the OOK only transmits 15,000 bits in the data frame.

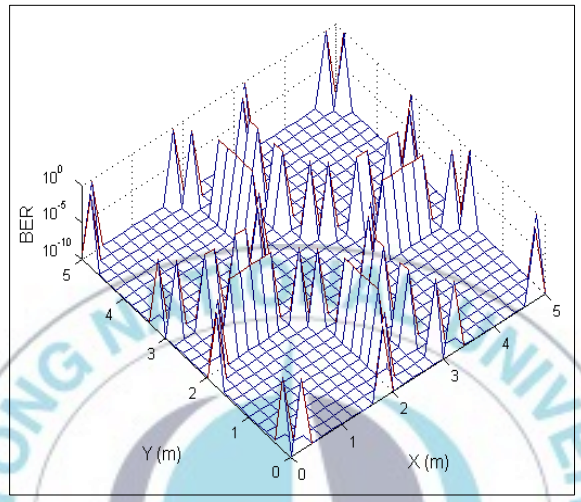

(a)

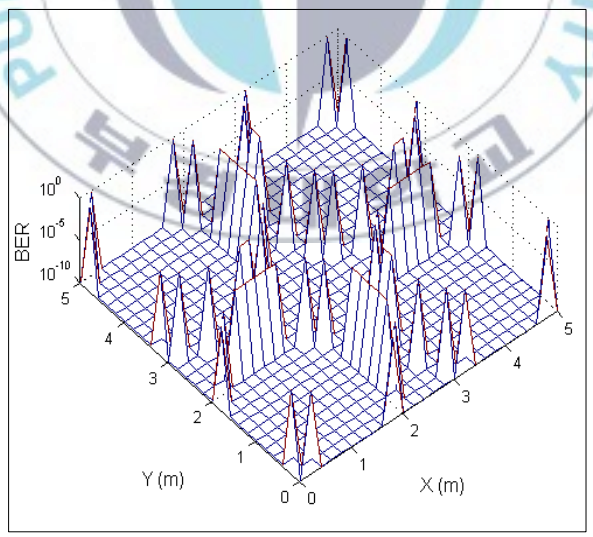

(b)

Figure 3.7. Distribution of BER over the working plane for (a) 4-PAM and (b)OOK.

Figure 3.7(b) shows the BER distribution over the working plane with OOK transmission. In this modulation scheme, the maximum BER is found to be 0.5026 and the minimum is 10^{-10}, and the average BER is 0.0467.

The performance comparison of two modulation schemes is summarized in Table 3.1.

Table 3.1. Summary of results

Modulation	Number of data bits	TS length	Data rate	Minimum BER	Average BER	Maximum BER
OOK	15,000	500 bits	500Mbps	10^{-10}	0.0467	0.5026
4-PAM	30,000	500 bits	1Gbps	10^{-10}	0.0501	0.5000

It can be seen that two BER distributions of 4-PAM and OOK are similar, due to the fact that the adaptive equalization performs in an optimum manner. We note, however, that the actual data rate of OOK is 500Mbps whereas the 4-PAM achieves 1Gbps, while the transmission rate of both systems is 500Msymbols/s. This is because, as mentioned earlier, we need to maintain the symbol rate at 500Msymbols/s in both cases, since the maximum LED switching speed is 500MHz.

We also analyze the outage area probability (OAP), i.e. the ratio of the area where BER is larger than 10^{-6} to the total service area. We observe the variation of OAP for different length of TS for both 4-PAM and OOK. With 4-PAM, the PD must be able to distinguish a larger number of intensity levels than OOK. Therefore, the error probability of optical/electrical conversion can be higher in 4-PAM. Figure 3.8 shows the results of the OAP comparison. We can see that the OAPs of 4-PAM are slightly higher than

those of OOK. For a 500 bit of TS length, the OAP with 4-PAM is 0.08876, whereas the OAP with OOK is 0.08284.

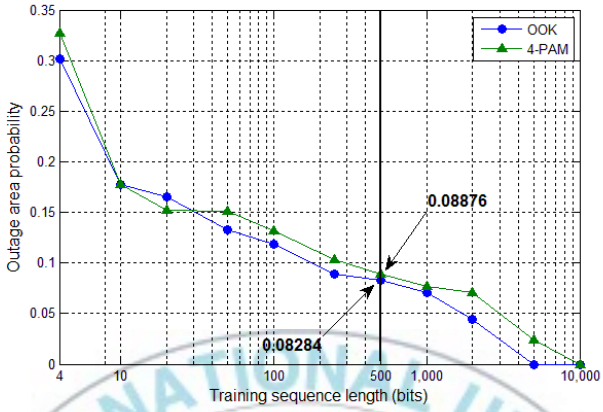

Figure 3.8. Outage area probability vs. training sequence length in bits.

Therefore, it can be concluded that for the same symbol rate, the throughput of the 4-PAM VLC with the RLS-DFE receiver can be significantly improved by a factor of 2, compared with that of OOK VLC with the RLS-DFE receiver. However, this gain is achieved at the expense of slightly increased OAP.

3.3. PAPR Reduction of OFDM in VLC

To overcome multipath effects, OFDM has been introduced for wireless communication systems. OFDM has also been used for VLC in many recent works [3, 22, 23], since it is a promising technique to reduce the ISI effects while increasing the data rate. In OFDM, the high-speed data stream is divided into several lower speed data streams and transmitted in parallel through several subcarriers. The subcarrier frequencies are assigned so that

they are within the channel delay spread limit. Therefore, the sub-channels is not affected by ISI, and the parallel transmission provides a high data rate.

However, OFDM inherently causes PAPR problem when the parallel data streams are summed up to create the OFDM signal. The peak power of the signal occurs when the subcarrier-modulated symbols are added in the same phase. A high PAPR value is an inherent disadvantage of OFDM and it causes nonlinear signal distortions and high power requirements for the transmitter amplifier. Hence in VLC, while using as transmitters, LEDs can be overheated by high power signal because of the limited voltage range and output power. Therefore, a thorough attention must be paid to this high PAPR problem when OFDM is used in VLC. Moreover, the voltage-to-current (V-I) relationship of LEDs shows a nonlinear behaviour which may distort the OFDM signal with high PAPR. Therefore, the high PAPR of the OFDM signal should be reduced before it is fed into transmitter LEDs.

Many techniques have been proposed to reduce the PAPR of OFDM systems in relation to RF baseband communication systems. Techniques such as clipping and filtering [24], block coding [25], selective mapping [26] and nonlinear companding transform (CT) techniques [27, 28] have been considered. Clipping techniques that used with OFDM [23, 29, 30] reduce large signals only or they hard-clip large signal peaks. This causes distortion noise that cannot be removed in the transmitted signal. Moreover, to reduce the high PAPR in VLC-OFDM, a DFT spread (DFTS) method has been proposed [31]. This DFTS method creates higher complexity in the system and offers a limited PAPR reduction. However, since the VLC-OFDM signal is a real-valued signal, the CT can be considered as a simpler method to reduce high PAPR in VLC-OFDM. In CT, the companding function is applied to the original OFDM signal so that it expands small signal

amplitude and compresses large signal amplitude. With the companding function applied, the average power of the signal can remain unchanged by using proper parameters for the companding function.

Several companding techniques such as μ-law companding [32], exponential companding [33], and error-function companding [28] have been proposed for the radio frequency (RF) baseband communication. This study considers μ-law companding and exponential companding that can be effectively used for VLC and we also propose a novel companding transform function.

3.3.1.PAPR in VLC-OFDM

Let the number of subcarriers be N and A_i be the i^{th} OFDM symbol. Then the time domain OFDM signal can be written as

$$s(t) = \sum_{i=0}^{N-1} A_i \exp\left(j2\pi \frac{i}{T} t\right), \qquad 0 \le t \le T. \tag{3.6}$$

Here, T is the symbol period. If this time domain signal is sampled at the rate of N/T and normalized by the factor of $1/N$, the time domain OFDM samples can be obtained as

$$s_n = \frac{1}{N} \sum_{i=0}^{N-1} A_i exp\left(j2\pi \frac{i}{N} n\right), \quad n = 0,1,2, \dots, N-1. \tag{3.7}$$

s_n has a real $\mathrm{Re}\{s_n\}$ and imaginary $\mathrm{Im}\{s_n\}$ parts and they can be considered as statistically independent and identically distributed (i.i.d.) random variables. Assume $\mathrm{Re}\{s_n\}$ and $\mathrm{Im}\{s_n\}$ are Gaussian-distributed with zero mean and with equal variances. Then the amplitude of the OFDM signal samples $|s_n|$ has a Rayleigh distribution and can be written as

$$|s_n| = \sqrt{Re^2\{s_n\} + Im^2\{s_n\}} \tag{3.8}$$

The PAPR of the discrete OFDM signal is the ratio of the maximum signal power to the average signal power, that is,

$$PAPR = \frac{max\{|s_n|^2\}}{E\{|s_n|^2\}}, \quad n \in [0, N-1]. \tag{3.9}$$

3.3.2.Principle of CT in VLC-OFDM

Let the companded signal be y_n. In VLC, the OFDM signal is a real-valued signal and the companding function is applied to the positive and negative amplitudes of the signal. Let the companding function be $f\ |s_n|$. Therefore,

$$y_n = f(|s_n|) \tag{3.10}$$

This real-valued companded signal is then fed to the LED. After passing through the channel, the received signal is obtained as

$$r_n = h_n y_n + w_n \tag{3.11}$$

Here, h_n is the samples of the channel impulse response and w_n is the channel noise. For simplicity, we ignore the channel impulse response and the received signal is obtained as

$$r_n = y_n + w_n \tag{3.12}$$

The original uncompanded signal can be reconstructed at the receiver by applying the inverse of the companding function, f^{-1}, to the received signal. The reconstructed OFDM signal is obtained as

$$\begin{aligned} \hat{s}_n &= f^{-1}(r_n) \\ &= f^{-1}(y_n + w_n) \end{aligned} \tag{3.13}$$

3.3.3.Nonlinear LED Model and VLC-OFDM System

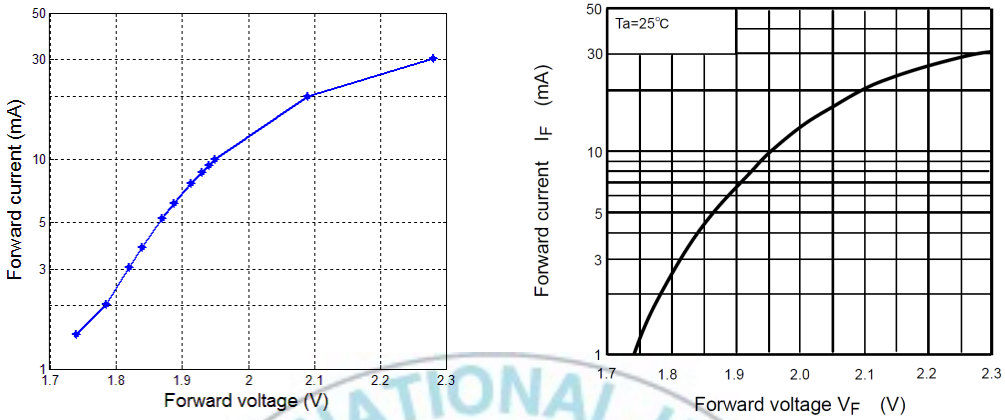

(a) (b)

Figure 3.9. V-I characteristic curves of the considered LED. (a) simulated curve (b) the curve from the data sheet.

For the simulations on VLC-OFDM, we transmit data using one LED. It has been previously proposed that InGaAlP based RCLEDs have a nearly 500MHz switching speed and it is suitable for high-speed VLC transmission [13]. Therefore, we consider the V-I characteristic curve of TOSHIBA TLSH160 LED lamp which is based on InGaAlP compound. As described earlier, the LEDs have nonlinear V-I characteristics. We model the nonlinear characteristic of the LED using curve-fitting technique. With a third degree polynomial, the curve-fitting technique could sufficiently match the V-I curve of the LED provided in the LED data sheet as shown in Figure 3.9.

The OFDM signal has a DC level at 0V. As it is shown in the characteristic curve, the LED operating voltage is approximately in the range of (1.75-2.3) V. Thus, the OFDM signal should be DC biased in order to

vary in the LED operating voltage range. We, therefore, add a DC bias voltage to the OFDM signal before it is fed into the LED.

In our simulation, we use 192 subcarriers, 8 pilot carriers, and 256-point FFT in the OFDM transmission system. To make the OFDM signal a real signal, we assign Hermitian symmetry (i.e. $X_n=X^*_{N-n}$) for the subcarriers [3]. Although this may lose a half of the bandwidth, it is not a considerable issue in VLC since VLC does not have limitations on bandwidth. After the Hermitian symmetric subcarriers are assigned for the IFFT operation, the output will be a real signal.

The block diagram of the VLC system is shown in Figure 3.10. In the transmitter, the generated data is passed through a convolutional encoder followed by an interleaver. Then the BPSK modulated data is added with pilot symbols and is processed by the IFFT operation. After the IFFT, the OFDM signal is generated and the cyclic prefix is also added. At this point, the OFDM may exhibit a high PAPR and thus we perform the CT at this stage as described previously. Therefore, the exponentially companded OFDM signal is fed to transmit through the LEDs.

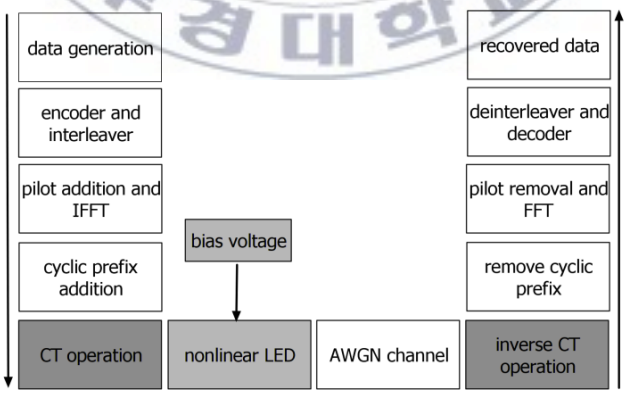

Figure 3.10. Block diagram of the VLC-OFDM system.

The transmitted data pass through the dispersive VLC channel and are received by the photo detector in the receiver. At the receiver, the inverse of the CT is performed in order to reconstruct the OFDM signal. Then the cyclic prefix is removed and FFT operation is performed. After removing the pilot symbols, data symbols are extracted and demodulated by BPSK demodulator. Data is regenerated after the de-interleaver and Viterbi decoder.

3.3.4.Application of CT Functions for VLC-OFDM

The study considers three CT functions for PAPR reduction in VLC-OFDM. The performances in VLC-OFDM are analyzed in terms of PAPR reduction capability and also subsequent BER performance. Over a companding process, the number of both low and high signal peaks is reduced and hence the probability of average power signal peaks increases. Therefore, over an appropriate range of signal power, the distribution of companded signal power becomes uniform.

3.3.4.1. μ-law CT

The μ-law CT is expressed as [32]

$$f(t) = k\ \mathrm{sgn}(t)\left[\frac{ln(1+\mu|t/k|)}{ln(1+\mu)}\right] \tag{3.14}$$

In (3.14), k is the mean amplitude of the input, whereas μ determines the shape of the transform function as in Figure 3.11. At the receiver, the inverse of the CT function is applied to remove any distortions made by the CT.

In the VLC-OFDM, the OFDM signal should be a real-valued signal, since the signal is transmitted via LEDs using IM. The μ-law CT is performed according to the VLC system block diagram in Figure 3.10.

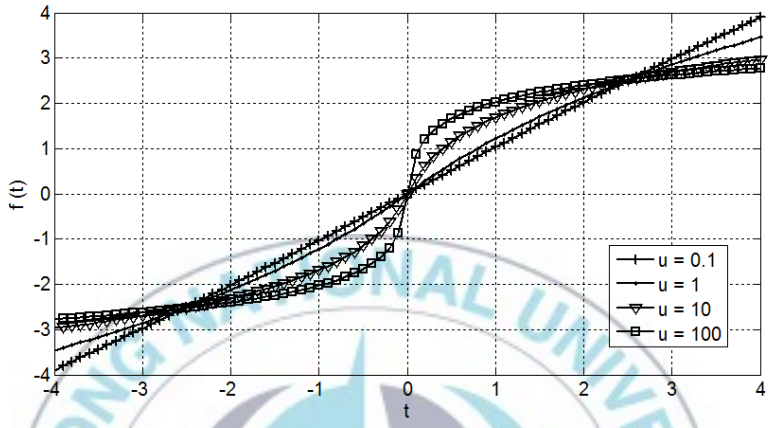

Figure 3.11. The curves of transform function with different μ values.

Performance Evaluation

In order to evaluate the PAPR reduction capability of the proposed companding function, we use the complementary cumulative distribution function (CCDF) of the probability of PAPR. The CCDFs of both uncompanded and the μ-law CT OFDM signals is depicted in Figure 3.12. It illustrates how the PAPR is affected by the value of μ. As seen in Figure 3.11, the shape of the CT function changes with μ. Therefore, the signal expansion and compression ratios change with μ, giving different PAPR reductions. It can be observed in Figure 3.12 that the PAPR reduction increases as the value of μ increases.

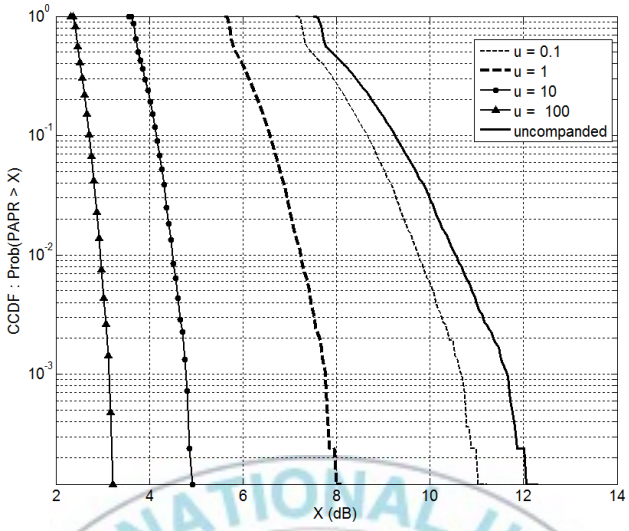

Figure 3.12. CCDFs of uncompanded signal and μ-law CT signal with different μ values.

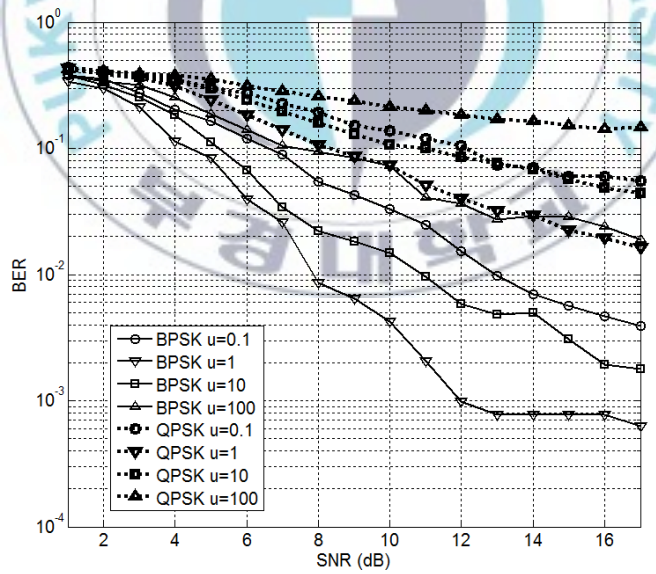

Figure 3.13**.** BER performance with μ-law CT for different values of μ.

We achieve nearly 3dB and 5dB PAPR at the CCDF of 10^{-3}, when μ is 100 and 10, respectively. To evaluate the BER performance of the indoor dispersive VLC-OFDM system, we choose a receiver position where there exists comparatively high delay spread from the rms delay spread in Figure 2.7. The rms delay spread at the chosen receiver position (1,1,0.85) is found to be 1.4ns.

The BER performance of the indoor VLC-OFDM system with the μ-law CT is evaluated and the results are shown in Figure 3.13. The system employs both BPSK and QPSK modulations over the indoor dispersive channel along with AWGN. The BER performances with μ = 1 and μ =10 are better than the ones with μ = 0.1 and μ = 100. However, as shown in Figure 3.12, it is important to note that a higher value of μ yields a higher PAPR reduction. Therefore, it can be concluded that there is a trade-off between PAPR reduction and BER performance in the VLC-OFDM system with the μ-law CT.

3.3.4.2. Exponential CT

Let $|y_n|^2$ be the squared magnitude of companded output and also assume it to be uniformly distributed over the interval [0,a], where a is an arbitrary value. Then, the cumulative distribution function (CDF) of $|y_n|^2$ can be written as [33]

$$F_{|y_n|^2}(x) = \frac{x}{a}, \qquad 0 \le x \le a \tag{3.15}$$

We can derive the CDF of $|y_n|$ using (3.15) as follows.

$$\begin{aligned} F_{|y_n|}(x) &= Prob\{|y_n| \le x\} \\ &= Prob\{|y_n|^2 \le x^2\} \end{aligned}$$

$$= \frac{x^2}{a}, \qquad 0 \le x \le \sqrt{a} \tag{3.16}$$

The inverse of $F_{|y_n|}(x)$ is then,

$$F_{|y_n|}^{-1}(x) = \sqrt{ax}, \qquad 0 \le x \le 1 \tag{3.17}$$

We can also derive,

$$\begin{aligned} F_{|s_n|}(x) &= Prob\{|s_n| \le x\} \\ &= Prob\{f(|s_n|) \le f(x)\} \\ &= F_{|y_n|}\big(f(x)\big) \\ &\qquad 0 \le x \le f^{-1}\big(\sqrt{a}\big) \end{aligned} \tag{3.18}$$

Therefore, from (3.18), we can obtain the companding function *f*(*x*) as

$$f(x) = F_{|y_n|}^{-1}\left(F_{|s_n|}(x)\right) \tag{3.19}$$

Substituting (3.17) for (3.19) and using the CDF of Rayleigh distribution, we can derive *f*(*x*) as

$$f(x) = \sqrt{a\left[1 - exp\left(-\frac{x^2}{\sigma^2}\right)\right]} \tag{3.20}$$

This is the exponential companding function. For the present study, this function is employed for reducing the PAPR.

In order for the average power level to remain unchanged during the companding operation, the value of *a* needs to be appropriately determined using

$$E\{|s_n|^2\} = E\{f^2(|s_n|)\} \tag{3.21}$$

That is, from (3.20) and (3.21), we can find

$$a = \frac{E\{|s_n|^2\}}{E\left\{1 - exp\left(-\frac{|s_n|^2}{\sigma^2}\right)\right\}} \tag{3.22}$$

Performance Evaluation

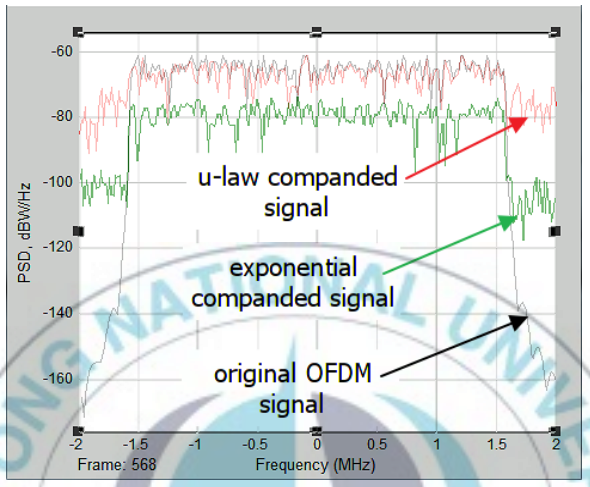

Figure 3.14. Power spectrum density (PSD) of original OFDM signal and other companded signals.

A salient feature of OFDM is that its power spectrum has a square-like shape. This is because of the high PAPR value of the OFDM signal. The OFDM power spectrum is affected by the companding transform [28, 33]. Usually, the power of out-of-band subcarriers is increased by the CT, while reducing the power of in-band subcarriers. Indeed, as shown in Figure 3.14, the two CT functions increase the out-of-band subcarrier power. However, it is found that the exponential companding transform increases the power of out-of-band subcarriers, compared with the original OFDM signal, but it is much less than the one from the μ-law companding.

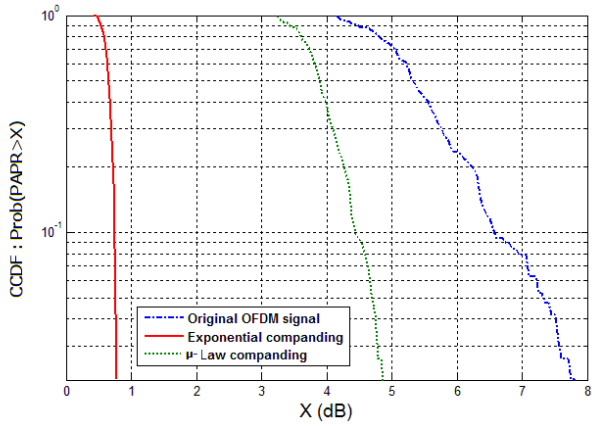

Figure 3.15. CCDF of PAPR of the original OFDM signal and other companded signals.

Figure 3.15 shows the CCDF of the PAPR values of the original OFDM signal, μ-law companded OFDM signal and the exponential function companded signal. It is demonstrated that while the μ-law companding transform somewhat reduces the probability of occurring high PAPR values, the exponential companding offers far superior capability of reducing the probability of having high PAPR values of the OFDM signal.

In addition, we have performed a comparative performance evaluation between the μ-law companding and exponential companding. Figure 3.16 shows the comparison of the BER performances. The simulation was done with the BPSK modulation. For both CT schemes, the average power of the signal was maintained nearly at the same value as before the companding. However, it is clear that the exponential companding technique outperforms the μ-law companding in terms of BER performance. It can be observed that a 2dB gain in terms of SNR values over the μ-law companding is obtained.

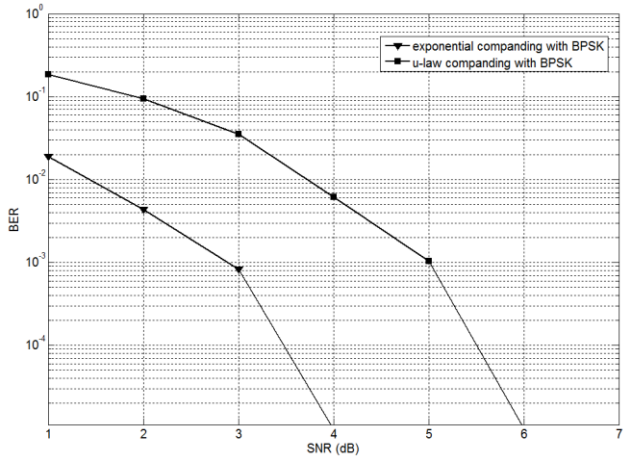

Figure 3.16. BER performances of μ-law companding and exponential companding techniques.

3.3.4.3. Novel CT

This study derives a novel CT function that is suitable for reducing PAPR in VLC-OFDM. In nonlinear CT schemes, large signal amplitudes should be compressed while expanding the small signal amplitudes. For this operation, the transform function should have the shape of a sigmoid curve, and it should be symmetric around the point (0,0) as seen in Figure 3.17. If the variable t is the input amplitude and $f(t)$ is the output amplitude, one clearly sees in Figure 3.17 that high input amplitudes are compressed at the output while low input amplitudes are expanded.

We start derivation of the proposed CT function with

$$f(t) = \frac{1}{1 + e^{-t}} \tag{3.23}$$

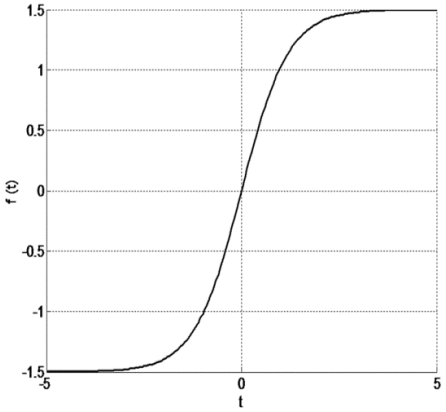

Figure 3.17. A symmetric sigmoid curve.

The inflection point of (3.23) is obtained using the second derivative which is calculated as

$$\frac{df(t)}{dt} = \frac{e^{-t}}{(1+e^{-t})^2}$$
$$\frac{d^2f(t)}{dt^2} = \frac{2e^{-2t}}{(1+e^{-t})^3} - \frac{e^{-t}}{(1+e^{-t})^2} \tag{3.24}$$

For $d^2f(t)/dt^2=0$, t gets the value 0. Hence, using (3.23), we can get $f(t)=0.5$ when $t=0$. That is, the inflection point of (3.23) is (0,0.5) which is not suitable for a CT function. In order to shift the inflection point to (0,0), we modify (3.23) as

$$f(t) = \frac{1}{1+e^{-t}} - 0.5 \tag{3.25}$$

In the proposed CT function, we made the signal compression and expansion weights independently changeable. In order to change the signal compression we introduce the parameter B as the compression weight that changes the gradient of (3.25) at the inflection point. And we also introduce

the parameter k that changes the maximum amplitude of the companded signal.

$$f(t) = k\left[\frac{1}{1+Be^{-t}} - 0.5\right] \tag{3.26}$$

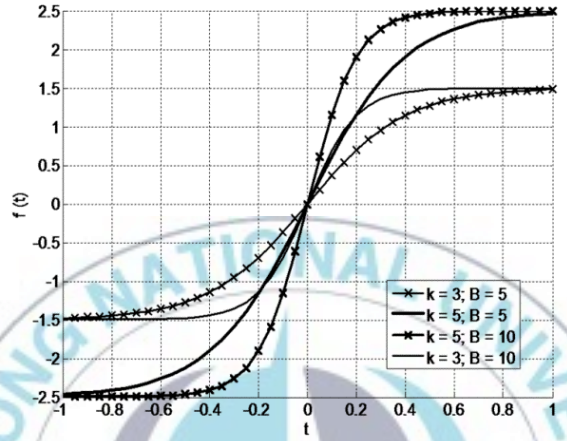

Figure 3.18. Curves of (3.26) with dependence between k and B.

However, as seen in Figure 3.18, B and k is not independent yet. Therefore, we make B and k independent in the proposed CT function $f_{CT}(t)$ as

$$f_{CT}(t) = k\left[\frac{1}{1+exp\left(-\frac{B}{k}t\right)} - 0.5\right] \tag{3.27}$$

In (3.27), the constant k determines the maximum signal amplitude or the compression level of large signals and the constant B determines the expansion level of small signals. With (3.27), these expansion and compression levels can be changed independently as seen in Figure 3.19. Also, it can be seen that large signal amplitudes are reduced while small

signal amplitudes are increased. At the receiver, we apply the inverse of the companding function, which is given in (3.28).

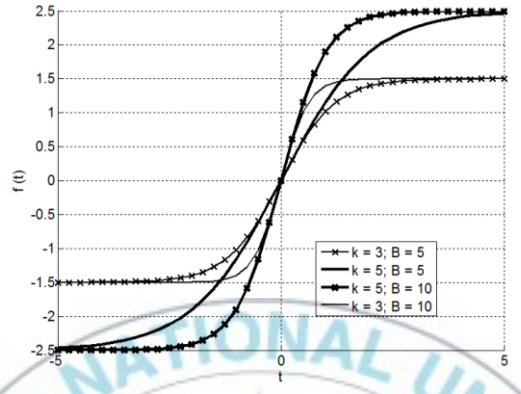

Figure 3.19. The proposed CT function with independent *k* and *B*.

$$f_{CT}^{-1}(t) = -\frac{k}{B}\ln\left[\frac{1}{\left(\frac{t}{k}+0.5\right)}-1\right] \tag{3.28}$$

In order for the average power of the companded signal to be the same as the uncompanded OFDM signal, we have to ensure $E\{|s_n|^2\}=E\{f_{CT}^2(|s_n|^2)\}$, where E is the expected value.

Therefore, (3.29) is obtained by substituting (3.27) for f_{CT}. Using (3.29), we can find values for k and B in order for the average power to remain unchanged.

$$E\{|s_n|^2\} = 0.25k^2 - k^2E\left\{\frac{1}{1+exp\left(-\frac{B}{k}|s_n|\right)}\right\} + k^2E\left\{\frac{1}{\left[1+exp\left(-\frac{B}{k}|s_n|\right)\right]^2}\right\} \tag{3.29}$$

Performance Evaluation

In this section, we evaluate the PAPR reduction performance and the BER performance of the proposed CT scheme over the μ-law and exponential CT schemes. In addition, although DFTS cannot be applied to the proposed system directly, we compare the performance with the results of DFTS method mentioned in [31].

The uncompanded and the companded OFDM signals depicted in Figure 3.20 show that the high signal peaks have been compressed while the small signal peaks have been expanded by the proposed CT.

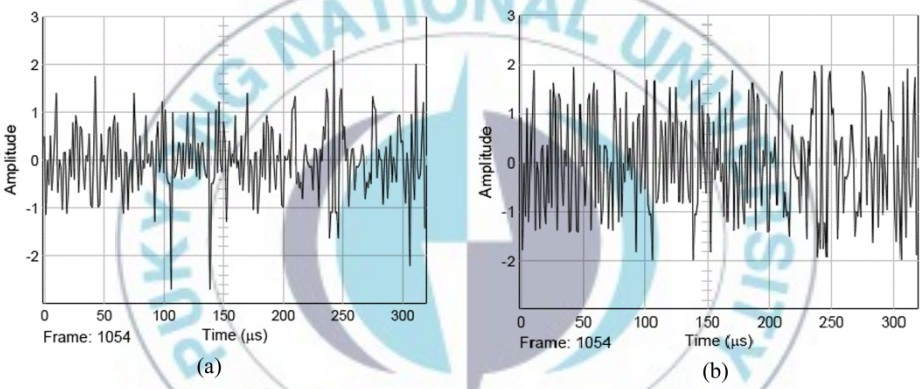

Figure 3.20. (a) Amplitude of the uncompanded OFDM signal, (b) The proposed CT signal.

The CCDFs of the signals are illustrated in Figure 3.21. It can be seen that the proposed CT achieves a significant PAPR reduction performance that is superior to that of μ-law and exponential CTs. At the CCDF value of 10^{-4}, for example, we achieve approximately 4dB PAPR with the proposed CT. However, with the μ-law and exponential CTs, the achieved PAPR values are nearly 7.5dB and 5dB, respectively. Moreover, that PAPR achieved by the proposed CT is nearly half of the PAPR the DFTS method

obtained. Therefore, the PAPR reduction capability of the proposed CT function for the VLC-OFDM is the best, compared with that of μ-law and exponential CTs and DFTS method.

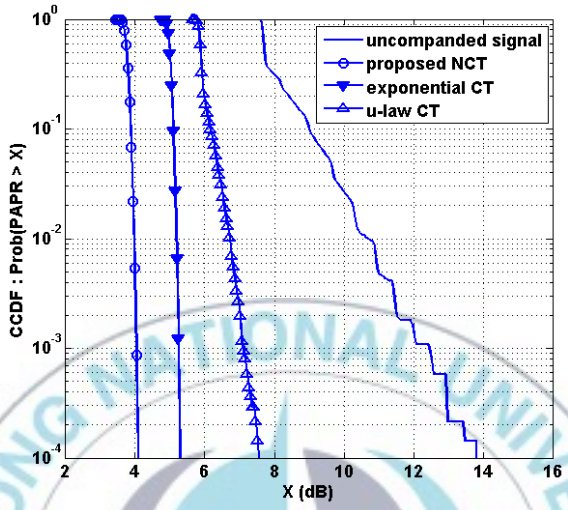

Figure 3.21. CCDF of the uncompanded signal, exponential CT signal, μ-law CT signal and proposed CT signal.

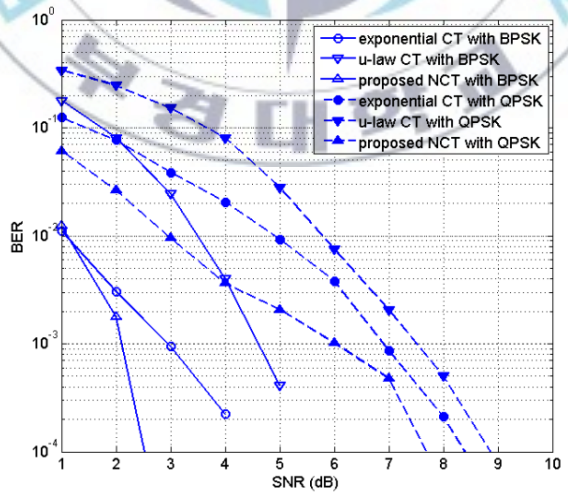

Figure 3.22. BER performance of the VLC-OFDM system with μ-law CT, exponential CT and proposed CT under AWGN.

The BER performance of the proposed VLC-OFDM system is also evaluated with BPSK and QPSK under the AWGN channel. The results of the performance analysis are shown Figure 3.22.

With the proposed CT, we convincingly achieve better performance than with μ-law and exponential CTs. In comparison with the previous study with DFTS, we also achieve a SNR value of nearly 7.5dB with QPSK and nearly 2.5dB with BPSK at the reference BER of 10^{-4}, whereas the DFTS method needs a SNR value of 17 dB for the same reference BER value.

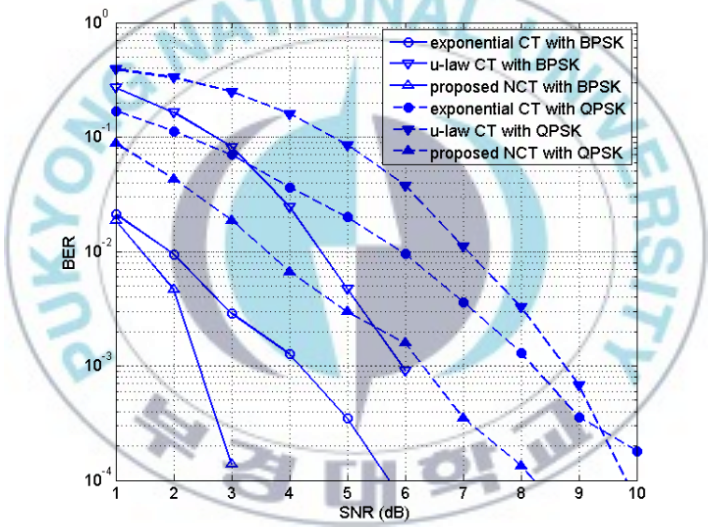

Figure 3.23. BER performance of the VLC-OFDM system with μ-law CT, exponential CT and proposed CT under the dispersive indoor channel

Since we design the VLC-OFDM system for an indoor environment, it is crucial to study the performance of the proposed VLC-OFDM system under the indoor dispersive channel. We consider the rms delay spread as the measure of the channel dispersion and according to the Figure 2.7, it can be seen that the rms delays spread depends on the position of the receiver. We

choose the receiver position (1,2,0.85) where there is an average rms delay spread of approximately 1.1ns. We analyze the BER performance at the chosen receiver position in Figure 3.23.

According to Figure 3.23 as well it can be verified that the proposed CT outperforms the previously proposed μ-law and exponential CTs in terms of the BER performance. Comparing with the results with DFTS method also, it can be clearly seen that the VLC-OFDM system gives a significant BER performance even under the dispersive indoor channel.

Therefore, it can be concluded that the VLC-OFDM system with the proposed CT offers the best BER performance as well as superior PAPR reduction capability.

3.4. Color-Clustered Multi-User VLC

With extensive researches and developments conducted over a decade, VLC systems have largely been focused on providing point-to-point communication links with substantial performances [1, 4].

However, as a wireless broadband communication technology, VLC should have an efficient MU access scenario in order to support the demand for the simultaneous network access. Recently, the MU-VLC has been addressed at aspects of controlling intensity with the aid of channel control, optical codes or protocol in the MU scenario. Z. Wang *et al*. [35] proposes a circular arrangement of LED on the room ceiling, so that the SNR variation for different locations in the room is reduced up to 0.9dB. Wang verifies that using this LED arrangement, all the users in the indoor environment can obtain almost the same communication quality regardless of their locations. They contend that the reduction in SNR fluctuation would be used for MU-VLC systems. An MU-VLC transmission scheme using Ethernet-optical

CDMA (OCDMA) has also been proposed by M. Guerra *et al*. [36]. Random optical codes (ROC) as the base for OCDMA to transmit data from multiple sources have been employed. An experimental setup showed that the Ethernet-OCDMA is suitable for multiple access in VLC. Wu *et al*. proposes two communication protocols to support multiple access in LOS VLC links [37]. Using the proposed protocols they reduce the LOS blocking in optical paths that is used by multiple nodes. In [38], Higgins et al. presented a genetic algorithm for channel control in MU-OWC. This algorithm controls the intensity provided to each spot in the diffuse environment, thereby offering a negligible effect of rms delay spread.

Recognizing the sufficient bandwidth of VLC, multiple users are allocated using different spectral bands in MU-VLC. In [39], Uddin *et al*. suggested a resource allocation method utilizing the visible light spectrum. That is, it allocates different user data in different spectral bands within the visible light spectrum, depending on the priority of the users. However, Uddin *et al*. did not present a MU detection scheme for the proposed MU scheme. In order to have a practically deployable MU-VLC system, a reliable MU detection scheme that is an essential part of the system must be provided.

Although the above mentioned studies address some aspects of the MU-VLC, a more comprehensive and complete VLC system is yet to be reported for an MU-VLC that offers wireless access as well as illumination.

In this study, we present a novel color-clustered user allocation technique and consequent user detection technique for indoor MU-VLC systems. The motivation to the idea of color-clustered MU scheme is that the entire spectrum of the visible light band is utilized and thus the spectral wastage in VLC can be minimized. The main principle of the color-clustering of

multiple users is that the users are assigned to the three primary colors; red, green and blue (RGB). Therefore, the users are clustered into specific visible spectral bands known as colors. The IM user data are transmitted via the red, green and blue beams of RGB light emitting diodes (RGB LEDs). Additionally, RGB LEDs are used to control the color of the indoor illumination.

The color-clustered user separation is primarily performed using a color sensor at the receiver. The color sensor is able to identify red, green and blue colors individually, and it outputs individual voltages proportional to the intensity of each color.

We design the color-clustered MU scheme that is compatible with the indoor VLC system described in Chapter 2. Over different indoor channel conditions and transmission scenarios, the proposed system is studied by simulations. The results of the simulations verify that the proposed indoor MU-VLC scheme provides significant performances while adequately ensuring indoor illumination.

3.4.1. User Allocation

A main advantage of visible light communication is its large unlicensed spectral range. This visible light spectrum starts from about 380 nm and goes up to about 740 nm. Most of the applications of VLC use single color LEDs (usually white LEDs) for data transmission and illumination. The modulation scheme known as CSK [40] is designed to exploit this wide spectral range for VLC in an efficient manner.

We employ this large spectrum to allocate different user data for a MU-VLC system. The different wavelengths (or colors) of light can be easily created with the RGB LEDs that produce red, green and blue colored beams

individually. When the R, G, B beams are produced in different intensities at the same time, the final output color of the RGB LED becomes a single composite color. In the color-clustered MU-VLC system, we allocate different users into these three primary colors defined as color clusters; cluster *r*, cluster *g* and cluster *b*. Using OOK, the data of the users in each cluster are intensity-modulated with red, green and blue beams of the RGB LED individually and transmitted simultaneously.

At the receiver, an RGB color sensor is used to detect the intensity of each beam. The color sensor produces separate voltages proportional to the detected R, G and B intensities, so that the users of each color cluster can be separated at the receiver.

Since there are only three color clusters, only up to three users can transmit data at a time. Therefore, in order to increase the user capacity of the proposed color-clustered MU scheme, we allocate more users in one color cluster by assigning specific intensity to each user within the allocated color cluster. However, since a single LED can produce a single intensity at a time, we use a set of LEDs with the specified intensity for every user in the system. That is, a particular set of LEDs is reserved to transmit data of a specific user. The user allocation scheme ensures that the specified color and the OOK intensity do not change within the specified LED set, as long as the user is connected to the VLC link. In this way, the user capacity can be significantly increased with an increased set of intensities. Figure 3.24 depicts a summary of the user allocation process. In Figure 3.24, we assume that the total number of users is three times the number of users within each color cluster, i.e. $N = 3K$.

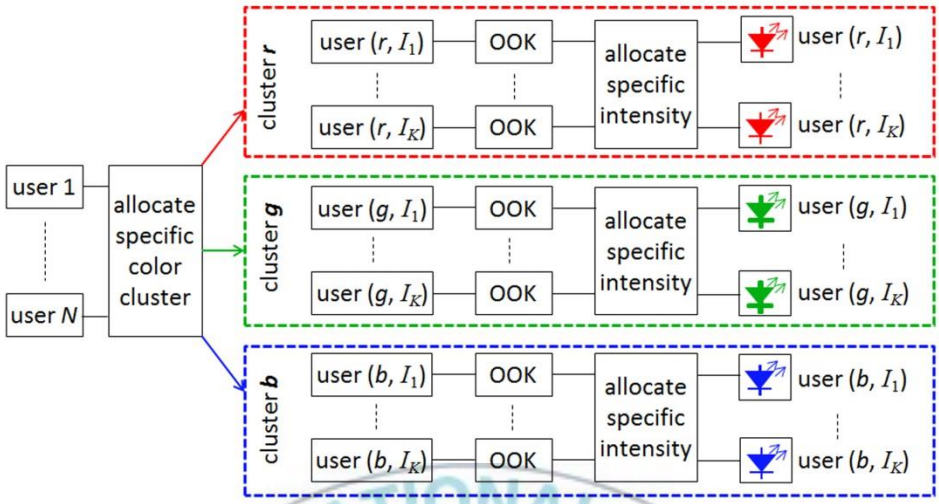

Figure 3.24. Color-cluster and intensity allocations of N users. K users are assigned into one color cluster ($N = 3K$).

3.4.2. MU Detection and User Separation

OOK modulation uses a low intensity for logic 0 (*off* state) and a high intensity for logic 1 (*on* state). As previously described, at the secondary user allocation stage, the users within a single color cluster are assigned with a specific intensity for the on state of the OOK, and the intensity of *off* state is kept the same for all users. The term user intensity is referred to the intensity of the *on* state of a particular user. The users within one color cluster transmit data through separate sets of LEDs simultaneously. The received intensity of each color can be identified using an RGB color sensor, which separately converts the RGB intensities into voltages. Therefore, the primary user separation is performed by the color sensor, extracting the composite signal in the particular user color from the received composite color beam.

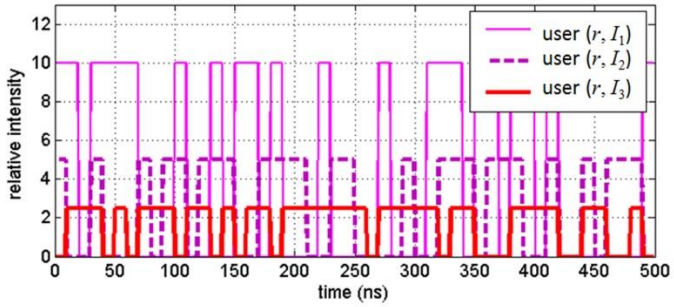

(a)

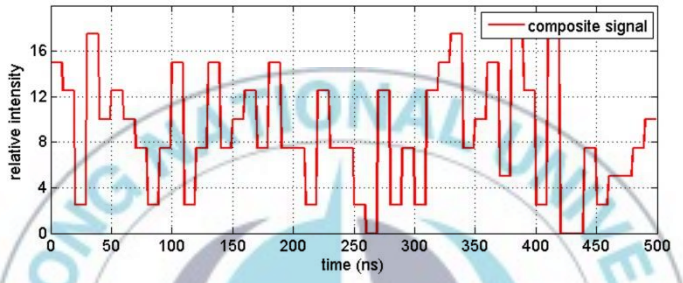

(b)

Figure 3.25. (a) OOK modulated data of the three users (b) the composite signal of the three users.

The secondary user data detection process is performed as follows. After the color sensor has extracted the cluster color, the received signal is a composite signal with added intensities of all users within the color cluster. Figure 3.25(a) shows the transmitted data of three users with relative intensities 10, 5 and 2.5 in cluster *r*. These intensities are relative to the intensity at *off* state. The composite signal made by adding individual user intensities of the three users is shown in Figure 3.25(b). The composite signal contains 8 intensities that are 17.5, 15, 12.5, 10, 7.5, 5, 2.5 and 0. To separate the users from this composite intensity, we propose the secondary user separation method.

Table 3.2. Look-up table for user separation from the received signal intensity (RSI) in one cluster.

user	OOK state							
user (r,1)	on	on	on	on	off	off	off	off
user (r,1)	on	on	off	off	on	on	off	off
user (r,1)	on	off	on	off	on	off	on	off
RSI	17.5	15	12.5	10	7.5	5	2.5	0

If we consider K number of users within one cluster, the simultaneous transmission of three user signals results in a composite signal that has a maximum of 2^K intensities. As shown in Figure 3.25, if there are three users in the cluster r, there are 8 intensities in the composite signal. Since the LEDs transmit *on* or *off* state continuously, the composite intensity contains either logic 0 or 1 of each user. We note that the composite intensity can be tabulated according to the user data. As an example, Table 3.2 shows a look-up table of the composite intensity for the three users. It is apparent that according to the look-up table given in Table 3.2, there is the specific intensity of the composite signal where each user data is either *on* or *off* state. Analyzing the received composite intensity and with the aid of the look-up table, the each user's receiver can detect the user data. It is assumed that the number of users connected to each color cluster is known and therefore all the users sharing the same color cluster can readily create the look-up table in order to extract the user data.

In the presence of noise, however, this received composite signal can be distorted so that the intensities cannot be perfectly distinguished by the

receiver. In addition to the noise, the VLC channel can be dispersive and often causes the received signal to be indistinguishable. In order to highlight the composite signal affected by the noise, we assigned two sets of user intensities to the three users; one with high separation between relative user intensities {10, 5, 2.5} and the other with low separation {4, 2, 1}. Figure 3.26 shows the vulnerability of the composite signal to the noise with the two user intensity sets. It is apparent that the composite signal distortion becomes lower if there is a higher intensity separation between user signals. In other words, the higher intensity separation makes it easier for the receiver to extract the composite intensity levels. This, in turn, will lead to reduce the BER of the user data.

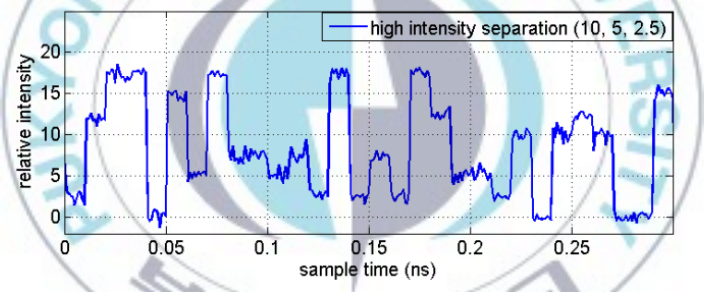

(a)

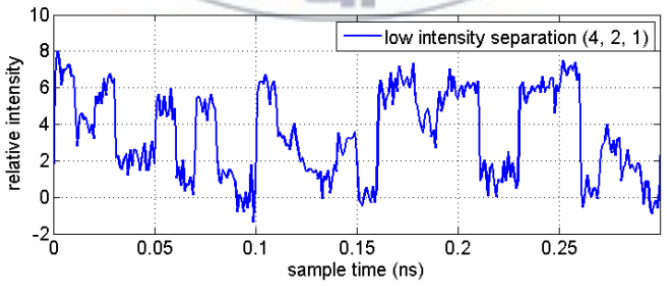

(b)

Figure 3.26. (a) Received composite signal with high user intensity separation (b) low user intensity separation at a SNR value of 5dB.

In order to reduce the distortion caused by channel-induced dispersion in the composite signal, the receiver needs to employ an equalizer. To this end, the present study employs a DFE in the receiver, where the equalizer adapts to channel variation over each location in the indoor environment. The RLS adaptive algorithm is used for the DFE, due to the fact that the RLS algorithm is characterized by the fast convergence of the adaptive filter coefficients and also proven to have substantial performances on high-speed indoor VLC systems in the previous experiments as well as [4]. For the RLS-DFE, we have used a training sequence of 500 symbols. The receiver structure of the MU-VLC is depicted in Figure 3.27.

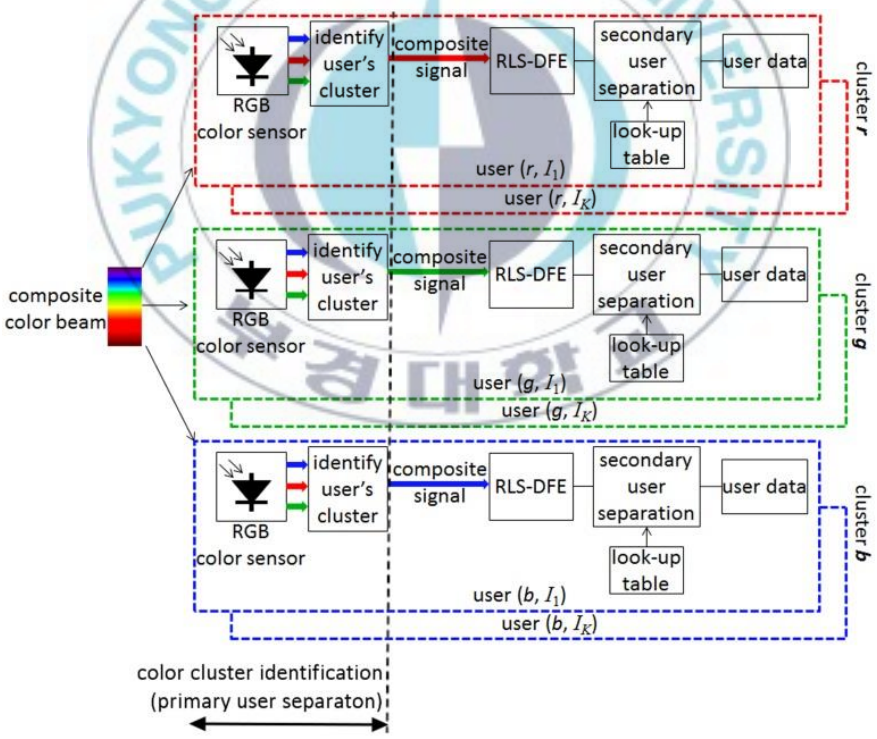

Figure 3.27. Structure of the receiver.

3.4.3. MU-VLC Transmitter Design

In general, an indoor VLC system should fulfil the three main functionalities: 1) to provide indoor illumination and communication simultaneously, 2) to provide required color and brightness, 3) to avoid color and intensity flicker. In order to satisfy these three basic requirements, we propose the MU-VLC transmitter with the following design criteria.

We designed the MU scheme that is applicable for the indoor VLC system that Chapter 2 described. In contrast to the previous experiments, in this study, we use transmitters that contain multiple RGB LEDs in each transmitter, in the same positions on the ceiling as shown in Figure 2.2. Each transmitter is designed so that, in one transmitter contains three sets of LEDs for the three color clusters. And in each color cluster, a subset of LEDs is allocated for one particular user as depicted in Figure 3.28. The number of subsets in one color cluster depends on the number of users connected to the VLC system at a given time. The modulation intensity of OOK in a single LED subset is fixed for a given user.

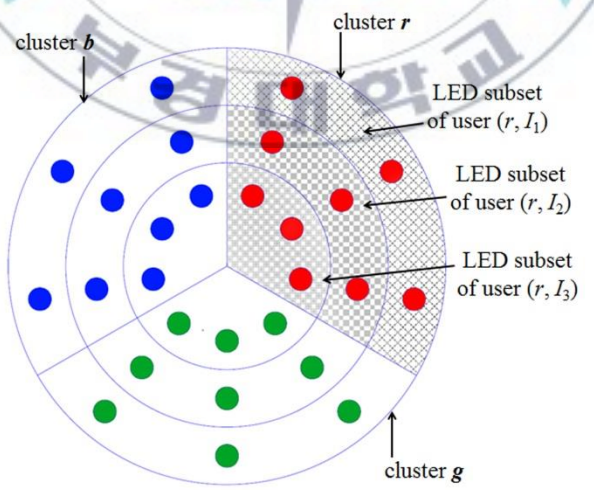

Figure 3.28. Transmitter design with multiple LEDs.

Consider a color cluster with RGB LEDs. As it was explained formerly, one cluster can be shared by several users. Because of the OOK transmission, the average power of one color varies rapidly in a particular cluster. This may cause color and intensity flicker in the indoor illumination, if the intensities of the other two colors are kept steady in a single LED. Therefore, we need to change the intensity of the other two colors according to the power variation of one color, in order to maintain a flicker-free constant color.

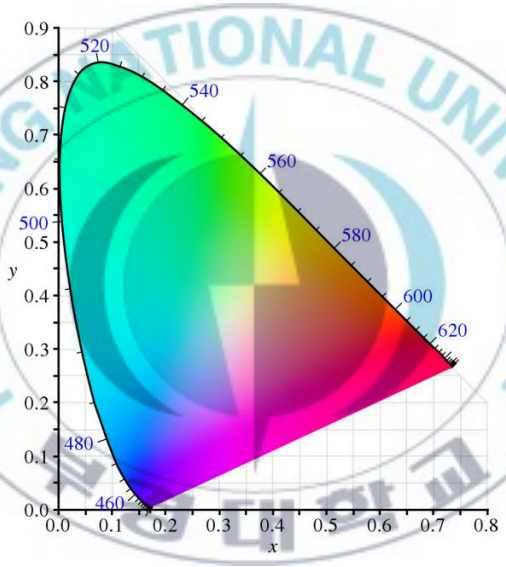

Figure 3.29. CIE 1931 color space chromaticity diagram.

According to International Commission on Illumination (CIE), the chromaticity of a specific color is given by the chromaticity coordinate diagram given in Figure 3.29 [41]. In order to provide a persistent color in the indoor illumination, we define the chromaticity coordinates of the desired output color as (x_p,y_p). Also, we define the chromaticity coordinates of the R, G, B values of a single LED as (x_r,y_r), (x_g,y_g) and (x_b,y_b), respectively. The

relative optical powers, P_r, P_g and P_b of R, G and B colors of a single LED, can be calculated using the following equations.

$$P_r x_r + P_g x_g + P_b x_b = x_p \tag{3.30}$$

$$P_r y_r + P_g y_g + P_b y_b = y_p \tag{3.31}$$

Let us consider the cluster r. The users who share the cluster r modulate data with the red beam of the LED. If the average transmitted optical power of one data frame of the k^{th} user, $k = 1, 2, 3, \ldots, K$, is $P_{avg(r,k)}$, the total optical power of one LED, $P_{tot(r,k)}$, can be given as

$$P_{avg(r,k)} + P_{g(r,k)} + P_{b(r,k)} = P_{tot(r,k)} \tag{3.32}$$

Here, the subscript (r,k) denotes the k^{th} user in the cluster r. Therefore, we can derive the total output power, P_{tot}, of all users in the cluster r as

$$P_{tot} = M \sum_{k=1}^{K} P_{tot(r,k)} \tag{3.33}$$

where M is the number of LEDs assigned per user and M is the same for all users. Since the intensity of an LED is proportional to the output power, we use the terms intensity and power interchangeably in this context. Let us consider a scenario where M is equal to be 1 and the user intensity of the k^{th} user of the cluster r is $P_{(r,k)}$. We must ensure that $P_{(r,k)}$ is always less than the maximum allowable output power of an LED. And we keep $P_{(r,k)}$ the same as long as the number of users within the cluster is unchanged, since the user detection method totally relies on $P_{(r,k)}$ value. In order to maintain a constant $P_{tot(r,k)}$ (3.32), the number of *on* and *off* states should be the same in every frame since $P_{avg(r,k)}$ depends on the number of *on* states per data frame. This

can be done using run length limited (RLL) line coding, so that the inter-frame intensity flicker can be mitigated [5]. In order to remove the color flicker, one can calculate the powers of green and blue beams in a single LED as follows.

$$P_{avg(r,k)}x_r + P_{g(r,k)}x_g + P_{b(r,k)}x_b = x_p \tag{3.34}$$

$$P_{avg(r,k)}y_r + P_{g(r,k)}y_g + P_{b(r,k)}y_b = y_p \tag{3.35}$$

$P_{g(r,k)}$ and $P_{b(r,k)}$ values are updated in every data frame prior to transmission. Finally, the VLC system is able to provide a color-controlled and flicker free transmission with final output color given by the color coordinates (x_p,y_p). We use this scheme for the flicker-free transmission to satisfy the functionality of illumination.

3.4.4.Performance Analysis of the MU-VLC System

We assume that the color sensor independently identifies red, green and blue colors. Hence, there is no user interference between color clusters. We simulate the user separation within one color cluster using the criteria described formerly. In the simulation, we assign three users per cluster. As mentioned previously, any number of users per cluster can be assigned with diminishing error performance because of a lower intensity separation.

We first study the MU-VLC transmission under the AWGN channel. Figure 3.30 shows the BER performance for three users in cluster *r* that have the intensities I_1=10, I_2=5.0, I_3=2.5. It can be observed in Figure 3.30 that all the users achieve a BER of 10^{-3} at the SNR values less than 8dB.

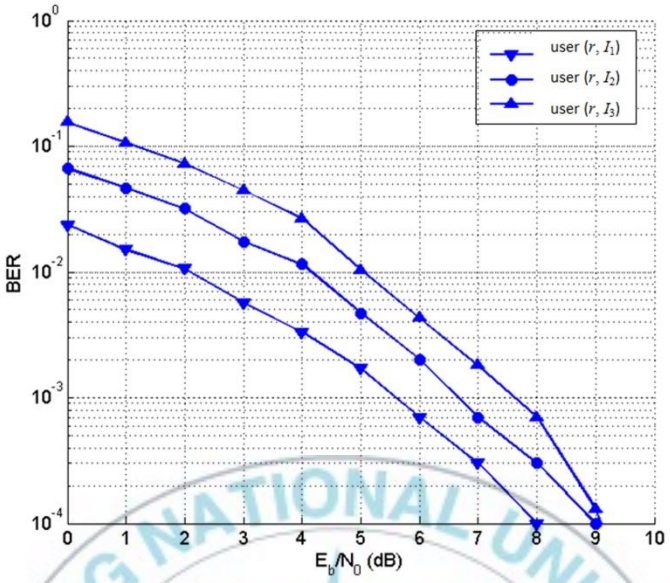

Figure 3.30. BER performance of the MU-VLC under AWGN.

However, since the MU-VLC system is designed for indoor environments, performances of the proposed system should also be thoroughly evaluated under the indoor dispersive channel model. As in Figure 2.7, since the rms delay spread varies according to the position of the user, the level of the composite signal distortion will vary at various receiver locations. Following the evaluation of the rms delay spread distribution, the average rms delay spread over the entire receiver plane is found to be approximately 1.1ns. Also, the minimum rms delay spread over the realistic receiver locations in the room is approximately 0.4ns. Hence, we study the BER performances of the MU transmission at these two values of rms delay spread. In the simulation, we use the same rms delay spread for all users at a time. The simulation results are shown in Figure 3.31. It is found that under a lower rms delay spread, the users can experience better BER performances due to lower channel dispersion.

According to Figure 2.7, most of the indoor area exhibit the rms delay spread ranging from 1.0ns to 1.2ns. Therefore, the results of Figure 3.31 show that all the users can receive BER values better than 10^{-3} in most of the area when the SNR value is greater than 7dB.

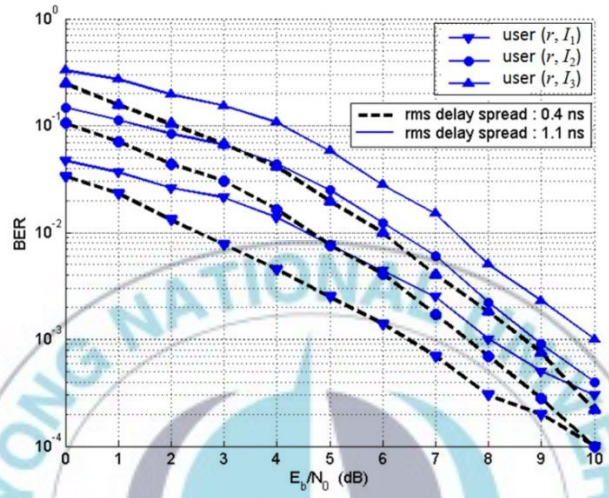

Figure 3.32. BER performance with the rms delay spread values of 0.4ns and 1.1ns. The relative user intensities (I_1,I_2,I_3) are {10, 5, 2.5}.

Moreover, when the dispersive channel performance (Figure 3.31) is compared with the AWGN performance (Figure 3.30), it can be observed for user (r,I_3) that the BER degradation due to the channel dispersion of 1.1ns is approximately 0.0019 at 9dB SNR. This means that the MU-VLC system is able to provide a reliable communication link even under relatively high channel dispersion.

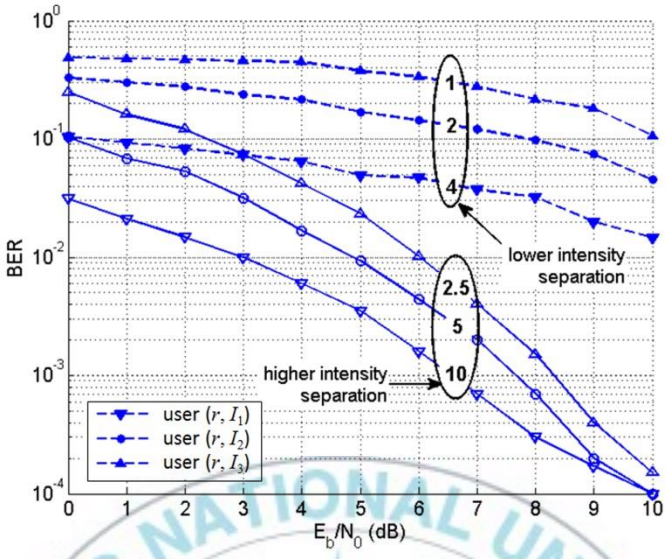

Figure 3.32. BER performances of the users with different relative intensities at an rms delay spread value of 0.4ns.

As shown earlier, the composite signal distortion stems from not only the delay spread but also the relative intensity separation (see Figure 3.26). Therefore, the BER performances of the users would vary with different user intensity separation. We assign the three users with a set of relative intensities {4, 2, 1} and another set of intensities {10, 5, 2.5}. The BERs of the users under these two intensity sets are compared in Figure 3.32. It can be clearly seen that the users having a higher intensity separation produce much lower BERs than the users having a lower intensity separation. Moreover, a user with a higher intensity within the set shows a lower BER and hence experiences better communication quality even at lower SNR values. Nevertheless, convergence can be observed in the BERs of all users at higher SNR values, since the composite signal would experience a lower distortion with increasing signal power.

With the results shown in Figures 3.30, 3.31 and 3.32, we can draw conclusions that the proposed indoor MU-VLC system with the color-clustered MU scheme is able to provide significant performance.

4. Conclusions

In this thesis, a design of a MU-VLC system that uses LEDs is studied for high-speed data communication. The study is conducted with four major experiments undertaken at various aspects of VLC. An indoor channel model is considered for investigation the effect of the channel dispersion on the transmission. The underlying indoor VLC system is fundamentally evaluated for received signal strength for optical wireless data communications and adequate indoor illumination in compliance with ISO standards.

In the first study, to overcome the multipath induced ISI problem in indoor VLC, we evaluate performances of RLS-DFE which requires a training sequence to achieve the elimination of ISI. The use of the training sequence lowers the energy efficiency as well as throughput. We evaluate the RLS algorithm to reduce the training sequence length. It is found that 500 bits long training sequence is only necessary for a data rate of up to 1Gbps to adapt the equalizer. This will greatly improve energy efficiency and throughput of the VLC system.

Secondly, we have considered a high rate and high throughput VLC system with inherent LED limitations such as LED switching speed and photo detector conversion rate. The proposed system employs the 4-PAM scheme and the RLS-DFE receiver. Performance analysis shows that the proposed system can transmit a data rate up to 1Gbps in compliance with the LED switching speed of 500MHz. Also, the outage area probability analysis shows that it can deliver nearly error-free transmission for most parts of the environment at 1Gbps with the TS of 500 bits long. Therefore, in comparison with the OOK based transmission scheme, the proposed system offers a higher data rate as well as higher throughput, while both schemes meet the LED switching speed limitation.

In the third study, we address the issue of a high PAPR of OFDM signal when used in VLC. The high PAPR in the VLC-OFDM signals distorts the transmitted signals, due to the nonlinear V-I characteristics of the transmitter LEDs. To reduce these adverse effects in the indoor VLC-OFDM systems, we propose three CT schemes; μ-law CT, exponential CT, and CT.

It is demonstrated that in the μ-law CT scheme, the PAPR reduction capability increases with the value of μ. The results of the BER performance over an indoor dispersive channel model exhibit that the higher the value of μ is, the higher the BER will be. Therefore, the trade-off between the PAPR reduction strength and the BER performance should be taken into account for the μ-law CT based VLC-OFDM systems.

With the use of exponential CT, computer simulations demonstrate that the PAPR of VLC-OFDM is considerably reduced. In addition, its BER performance and power spectrum show superiority over the μ-law companding function that is proposed in the previous study. Therefore, the exponential companding technique is proved as a better scheme suited to the real-valued VLC-OFDM signal than μ-law CT, for reducing high PAPR problems and for a better BER performance.

A novel CT function is proposed as the third CT. Comparative studies show that the proposed CT function provides the most significant PAPR reduction performance and offers the most superior BER performance as well. Therefore, the proposed CT and subsequent VLC-OFDM system would facilitate efficient OFDM signal transmissions via the LEDs that have nonlinear electrical/optical characteristics and limited operating voltage range.

In the final study, a novel color-clustered MU scheme is proposed for indoor MU-VLC systems. The proposed MU-VLC scheme allocates users

into separate spectral bands defined as red, green and blue color clusters. The user data are transmitted by IM with the light beams with particular cluster color. In order to increase the user capacity of the MU system, we assign specific user intensities for the users within a color cluster. Apart from the capacity and performance offered by the proposed MU-VLC system, sufficient illumination and flicker-free effect are also ensured. Under various transmission scenarios such as channel dispersion and noise, the simulation results demonstrate that the proposed system performs well, offering increased performance over most of the area in an indoor room. It is found that the users having higher relative intensity achieve lower BERs. As the signal power increases, however, all users are able to achieve relatively similar performances. Due to LED power limitation, the number of users within a color cluster would be limited. It would be, therefore, interesting to analyze the user capacity on a heavy demand for multiple access.

References

[1] T. Komine, M. Nakagawa, “Fundamental analysis for visible-light communication system using LED lights,” IEEE Transactions on Consumer Electronics, vol. 50, no. 1, pp. 100-107, Feb. 2004.

[2] S. Haruyama, “Visible light communication using sustainable LED lights”, Proceedings of ITU Kaleidoscope: Building Sustainable Communities, pp. 1-6, April 2013.

[3] F.M. Wu, C.T. Lin, C. Wei, C.W. Chen, “Performance Comparison of OFDM Signal and CAP Signal Over High Capacity RGB-LED-Based WDM Visible Light Communication”, Photonics Journal, IEEE, vol. 5, no. 4, 2013.

[4] K. Bandara, Yeon-Ho Chung, “Reduced training sequence using RLS adaptive algorithm with decision feedback equalizer in indoor visible light wireless communication channel,” 2012 International Conference on ICT Convergence, pp. 149-154, October 15-17, 2012.

[5] S. Rajagopal, R. Roberts, S. Lim, “IEEE 802.15.7 visible light communication: modulation schemes and dimming support,” IEEE Communications Magazine, vol. 5. no.3, March 2012.

[6] U. Sethakaset and T.A. Gulliver, “Differential amplitude pulse-position modulation for indoor wireless optical communications,” EURASIP Journal on Applied Signal Processing, vol. 2005, pp. 3-11, 2005.

[7] D. Zwillinger, “Differential PPM has a higher throughput than PPM for the band-limited and average-power-limited optical channel,” IEEE Transactions on Information Theory, vol. 34, pp. 1269-1273, 1988.

[8] Dominic C. O'Brien, Lubin Zeng, Hoa Le-Minh, Grahame Faulkner, Joachim W. Walewski, Sebastian Randel, “Visible light communications: challenges and possibilities”, PIMRC, pp. 1-5, 2007.

[9] R.S. Berns, “Billmeyer and Saltzman’s Principles of color technology,” John Wiley & Sons Inc., 2000.

[10] J.M. Kahn, J.R. Barry, “Wireless infrared communications, ” Proc. IEEE, vol. 85, no. 2, pp. 265–298, 1997.

[11] Z. Ghassemlooy, W. Popoola, S. Rajbhandari, Optical Wireless Communications: System and Channel Modeling with MATLAB. Taylor & Francis Group: London, pp. 79, 2013.

[12] J.D. Parsons, “The Mobile Radio Propagation Channel,” Pentech Press Limited, London, pp. 184, 1992.

[13] Y. Tanaka,T. Komine, S. Haruyama, M. Nakagawa, "Indoor visible light data transmission system utilizing white LED lights", IEICE Trans. Commun, vol. E86B, no. 8, 2003.

[14] M.D. Audeh, J.M. Kahn, J.R. Barry, “Decision-feedback equalization of pulse-position modulation on measured nondirected indoor infrared channels,” IEEE Trans. Commun., vol. 47, no. 4, pp. 500-503, Apr. 1999.

[15] D.C.M. Lee and J.M. Kahn, “Coding and equalization for PPM on wireless infrared channels,” IEEE Trans. Commun., vol. 47, no. 2, pp. 255-260, Feb. 1999.

[16] Toshihiko Komine, Jun Hwan Lee, Shinichiro Haruyama, Masao Nakagawa, “Adaptive equalization for indoor visible-light wireless communication systems”, 2005 Asia-Pacific Conference on Communications, Perth, Western Australia, 3 - 5 October 2005.

[17] Ying Yi, Kyujin Lee, Yeong Min Jang, Jaesang Cha, Jin young Kim, Kyesan Lee, “Indoor LED-based identification systems using adaptive MMSE equalizer for optical multipath dispersion reduction”, ICTC, 2011, pp. 95-100.

[18] T. Komine, Jun Hwan Lee, S. Haruyama, M. Nakagawa, “Adaptive equalization system for visible light wireless communication utilizing multiple white LED lighting equipment”, IEEE Trans. Wireless Commun., vol. 8, no. 6, pp. 2892-2900, June 2009.

[19] T.S. Rappaport, “Wireless communications: principles and practice”, 2nd edition. Prentice Hall PTR, 2002.

[20] K. Takaoka, and G. Hatakoshi, “InGaAlP-based red VCSEL & RCLED,” IEICE Technical Report, vol. LQE2000-128, pp. 51-56, 2001.

[21] Kang-Il Ahn, Jae Kyun Kwon, “Capacity Analysis of M-PAM Inverse Source Coding in Visible Light Communications,” Journal of Lightwave Technology, vol. 30, pp. 1399- 1404, May 2012.

[22] Y. Tanaka, T. Komine, S. Haruyama, and M. Nakagawa, “Indoor visible communication utilizing plural white LEDs as lighting,” 12th IEEE International Symposium on Personal, Indoor and Mobile Radio Communications, pp. F81–F85, Sept., Oct. 2001.

[23] H. Elgala, R. Mesleh, H. Haas, “An LED model for intensity-modulated optical communication systems,” IEEE Photonics Technology Letters, vol. 22, no. 11, pp. 835-837, June 2010.

[24] J. Akhtman, B. Z. Bobrovsky, and L. Hanzo, “Peak-to-average power ratio reduction for OFDM modems,” The 57th IEEE Semiannual Vehicular Technology Conference, vol. 2, Apr. 2003, pp. 1188–1192.

[25] A. E. Jones, T. A. Wilkinson, and S. Barton, “Block coding scheme for reduction of peak to mean envelope power ratio of multicarrier

transmission schemes," IEEE Electron. Letters, vol. 30, no. 25, pp. 2098–2099, Dec. 1994.

[26] R. W. Bami, R. F. H. Fischer, and J. B. Hber, "Reducing the peak-to-average power ratio of multicarrier modulation by selective mapping," IEEE Electron. Letters, vol. 32, pp. 2056–2057, Oct. 1996.

[27] X. Wang, T. T. Tjhung, and C. S. Ng, "Reduction of peak-to-average power ratio of OFDM system using a companding technique," IEEE Trans. Broadcast., vol. 45, pp. 303–307, Sep. 1999.

[28] T. Jiang and G. Zhu, "Nonlinear companding transform for reducing peak-to-average power ratio of OFDM signals," IEEE Trans. Broadcast., vol. 50, pp. 342–346, Sep. 2004.

[29] D. Guel, Palicot, Jacques, "Analysis and comparison of clipping techniques for OFDM peak-to-average power ratio reduction," 16th International Conference on Digital Signal Processing, pp. 1-6, 5-7 July 2009.

[30] Heung-Gyoon Ryu, Byoung-Ii Jin, In-Bae Kim, "PAPR reduction using soft clipping and ACI rejection in OFDM system," IEEE Transactions on Consumer Electronics, vol. 48, no. 1, pp. 17-22, Feb. 2002.

[31] S.B. Ryu, J.H. Choi, J. Bok, H.K. Lee, H.G. Ryu, "High Power Efficiency and Low Nonlinear Distortion for Wireless Visible Light Communication," Proc. IFIP International Conference on New Technologies, Mobility and Security, pp. 1-5, 2011.

[32] X. Wang, T. T. Tjhung, and C. S. Ng, "Reduction of peak-to-average power ratio of OFDM system using a companding technique," IEEE Trans. Broadcast., vol. 45, pp. 303–307, Sep. 1999.

[33] Tao Jiang, Yang Yang, Yong-hua Song, “Exponential companding technique for PAPR reduction in OFDM systems,” IEEE Transactions on Broadcasting, vol. 51, no. 2, pp. 244-248, June 2005.

[34] F.J. Richards, “A flexible growth function for empirical use,” Journal of Experimental Botany, vol. 10, no. 2, 290-301, 1959.

[35] Zixiong Wang, “A novel LED arrangement to reduce SNR fluctuation for multiuser in visible light communication systems,” 8th International Conference on Information, Communications and Signal Processing (ICICS), pp. 1 – 4, 13-16 Dec. 2011.

[36] M.F. Guerra-Medina, O. González, B. Rojas-Guillama, J.A. Martín-González, F. Delgado, J. Rabadán, “Ethernet-OCDMA system for multi-user visible light communications,” Electronics Letters, vol. 48, no. 4, pp. 227 - 228, April 2012.

[37] Z. Wu, “Network solutions for the line-of-sight problem of new multi-user indoor free-space optical system,” IET Communications, vol. 6, no. 5, March 2012.

[38] M.D. Higgins, R.J. Green, M.S. Leeson, “Genetic algorithm channel control for indoor optical wireless communications,” International Conference on Transparent Optical Networks, vol. 5, pp. 189-192, June 2008.

[39] M.S. Uddin, M.Z. Chowdhury Yeong Min Jang, “Priority-based resource allocation scheme for visible light communication,” Second International Conference on Ubiquitous and Future Networks, pp. 247-250, 2010.

[40] IEEE 802.15.7 Visible Light Communication Task Group. (2010, Aug. 30). IEEE 802.15 Documents.

[41] CIE (1932). Commission internationale de l'Eclairage proceedings, Cambridge: Cambridge University Press, 1931.

List of Publications

International Journals

[1] Kasun Bandara, P. Niroopan, Yeon-Ho Chung, “Improved Indoor Visible Light Communication with PAM and RLS Decision Feedback Equalizer,” IETE Journal of Research (SCIE), (to be published).

[2] Kasun Bandara, P. Niroopan, Yeon-Ho Chung, "On Companding Transform Techniques for OFDM Visible Light Communication over Indoor Dispersive Channels," Lecture Notes in Electrical Engineering (SCOPUS), (to be published).

[3] P. Niroopan, Kasun Bandara and Yeon-Ho Chung,“A User-Data Division Multiple Access Scheme,” Multimedia and Ubiquitous Engineering, Lecture Note in Electrical Engineering (SCOPUS), vol. 240, May 2013, pp. 849 – 855.

[4] P. Niroopan, Kasun Bandara and Yeon-Ho Chung, “Performance Improvement of IDMA System with High Resolution Signal Detection,” Journal of Next Generation Information Technology (JNIT), AICIT, vol. 4, no 2, April 2013, pp. 9-19.

[5] Kasun Bandara, Yeon-Ho Chung, “Novel Color-Clustered Multi-User Visible Light Communication,” Transactions on Emerging Telecommunications Technologies (SCIE), (in review).

[6] Khin Zar Chi Winn, Phyu Phyu Han, Kasun Bandara, “On the Performance of Quasi-Orthogonal Space Time Block Coded Massive MIMO with up to 16 Antennas,” Lecture Note in Electrical Engineering (SCOPUS), (in review).

International Conferences

[7] Kasun Bandara, Yeon-Ho Chung, "Reduced Training Sequence using RLS Adaptive Algorithm with Decision Feedback Equalizer in Indoor Visible Light Wireless Communication Channel," International Conference on ICT Convergence (ICTC), Jeju, South Korea, 15-17 Oct. 2012.

[8] Kasun Bandara, P. Niroopan, Yeon-Ho Chung, "PAPR Reduced OFDM Visible Light Communication using Exponential Nonlinear Companding," IEEE COMCAS 2013, Tel Aviv, Israel, 21 - 23 Oct. 2013.

[9] P. Niroopan, Kasun Bandara and Yeon-ho Chung, "A High Performance and Bandwidth Efficient IDMA Scheme with Large Receiver MIMO Technologies," The 4th International Conference on Mobile, Ubiquitous, and Intelligent Computing (MUSIC 2013), South Korea, Sept 2013.

[10] P. Niroopan, Kasun Bandara and Yeon-ho Chung, "A User-Data Division Multiple Access Scheme," International Conference on Green and Human Information Technology (ICGHIT), Hanoi, Vietnam, Feb 27 –Mar 1, 2013.

Domestic Conferences

[11] Kasun Bandara, P. Niroopan, Yeon-Ho Chung, "Effect of Reduced Training Sequence Length on Performance Improvement of Indoor VLC Systems," The conference of the Korean Institute of Communications and Information Science (KICS), South Korea, Dec. 2012, pp. 55-58.

[12] P. Niroopan, Kasun Bandara and Yeon-ho Chung, “On the Efficient Interleaver Design of Interleave Division Multiple Access” The Conference of the Korean Institute of Communications and Information Sciences (KICS), South Korea, Dec 8, 2012. pp. 103-106.

Workshops

[1] Kasun Bandara, “Visible Light Communication,” Korea – Japan Joint Workshop, Pukyong National University, Busan, South Korea, Sept. 24 -27, 2012.